UNIVERSITI KEBANGSAAN MALAYSIA
The National University of Malaysia

ANGKASA
INSTITUT SAINS ANGKASA
INSTITUTE OF SPACE SCIENCE

2012 ISWI & MAGDAS School
17-26 September 2012
Bandung, Indonesia

Sensing of upper and lower levels of the polar atmospheres using GPS

Wayan Suparta

Institute of Space Science (ANGKASA)
UNIVERSITI KEBANGSAAN MALAYSIA

Introduction

- The Global Navigation Satellite System (GNSS), particularly Global Positioning System (GPS) technology has become an essential tool in retrieving the ionospheric total electron content (TEC) and the atmospheric precipitable water vapor (PWV) at a low-cost, global scale covered and with superior temporal and spatial resolution through earth-based receivers.
- Presently, the intense development of TEC data from ground-based GPS receivers such used to monitor the ionospheric dynamics related to the space weather characterizing quantities (e.g. Jakowski et al., 2001; Cander, 2003), to detect the ionospheric response of strong earthquakes (Calais and Minster, 1995) and rocket launchings (Calais and Minster, 1996).

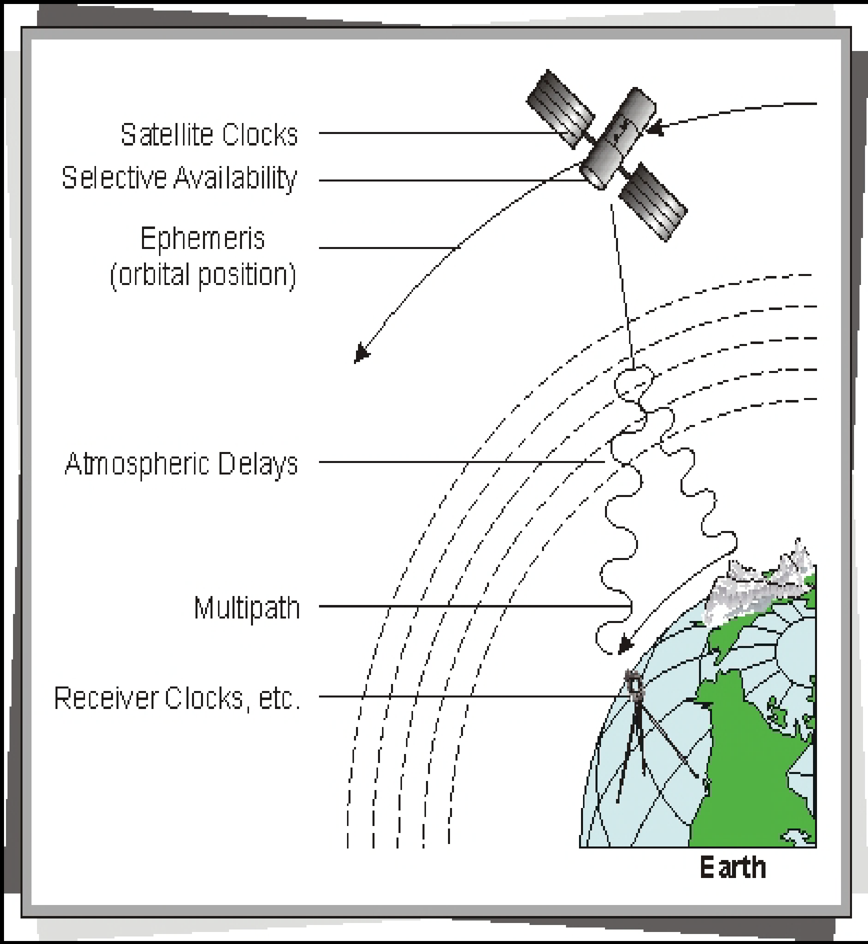

http://www.wirelessdictionary.com

- While PWV data developed were employed such as used for improving numerical weather forecast. In addition to the effective tool of GPS in various applications related to the Earth observation, an analysis of atmospheric structures and visualization of both tropospheric and ionospheric in real-time monitoring can help us to understand the connection processes between the solar activity and the terrestrial response.

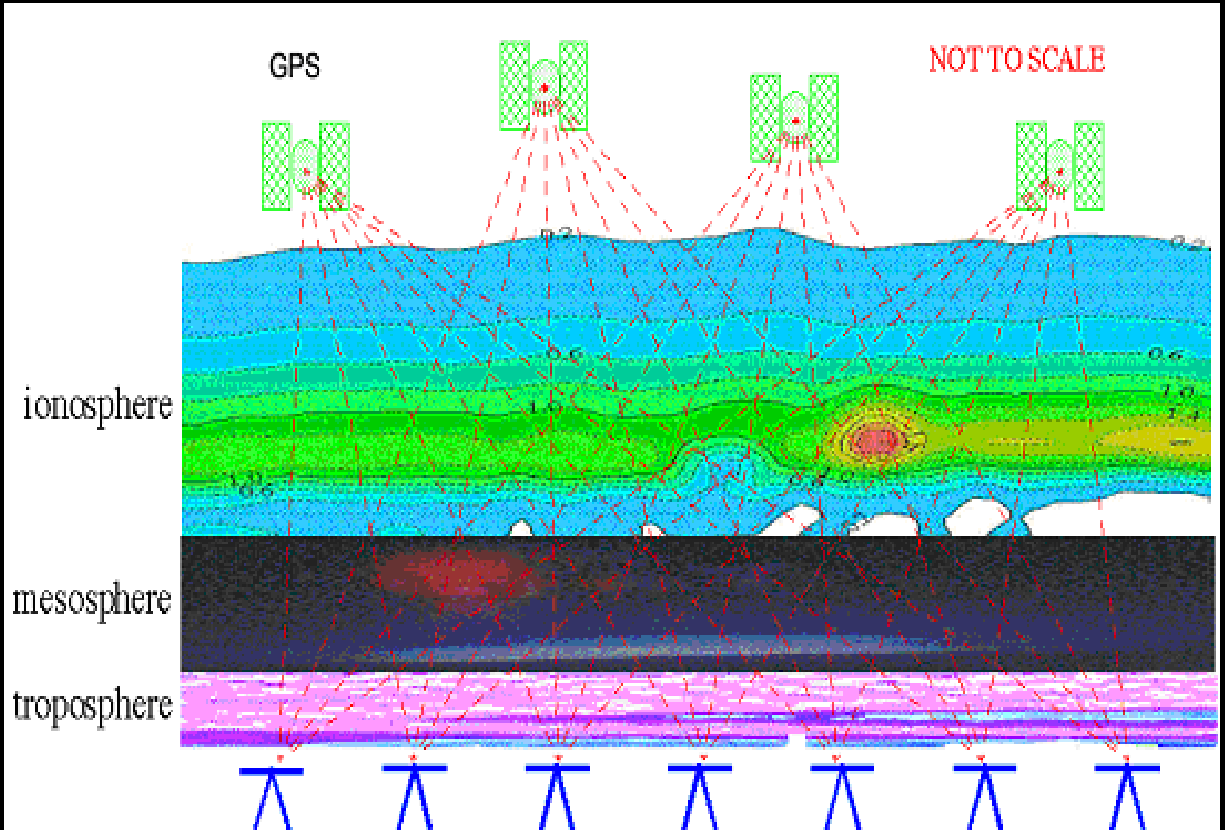

Ware et al. (2001)

- Therefore through the GPS measurements, the upper and lower levels of the atmosphere in Polar Regions are highlighted as an effort to gain knowledge and share the experience to establish the solar-climate relationship.

- Since the Polar Regions open as a natural laboratory for sensing the vast regions of near-Earth toward teleconnection between the upper and lower levels of the atmosphere, this talk addresses the determination of TEC and PWV from a GPS perspective.

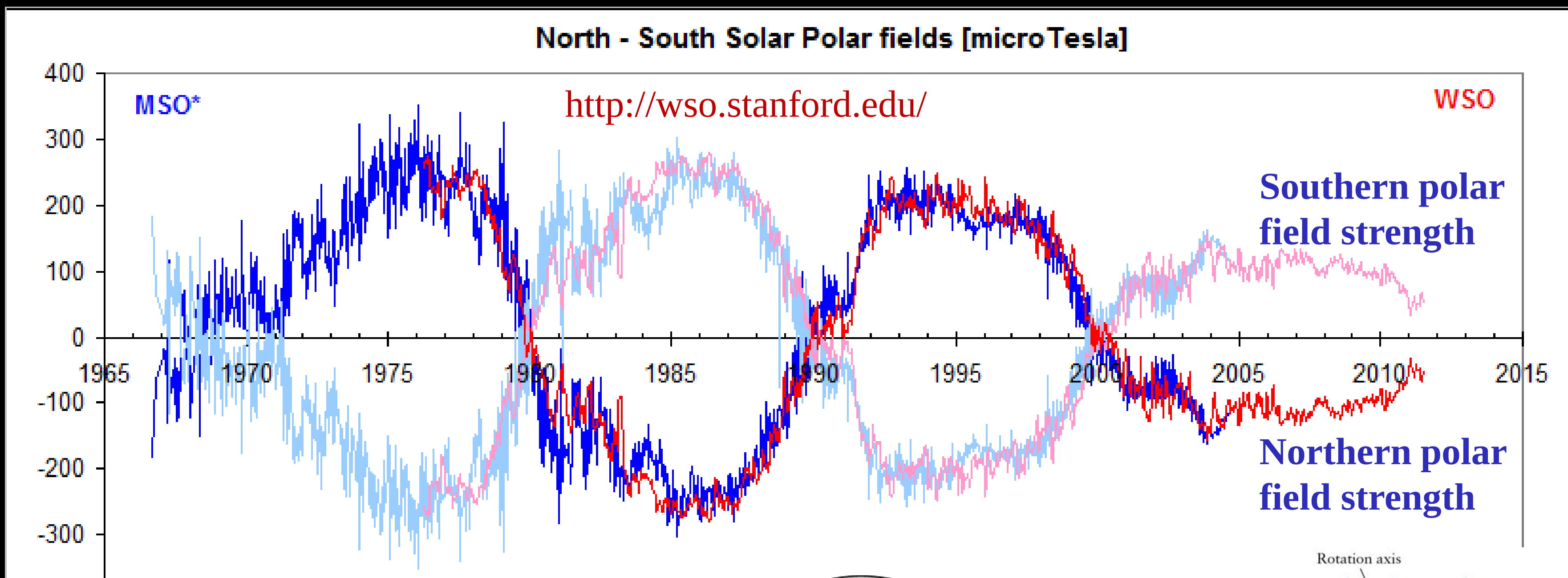

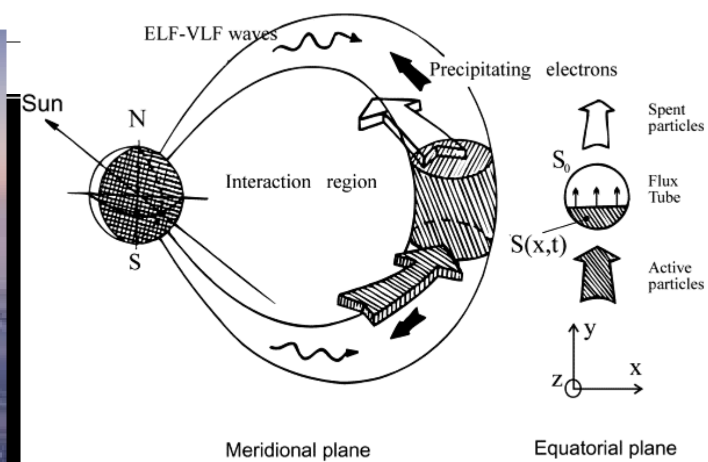

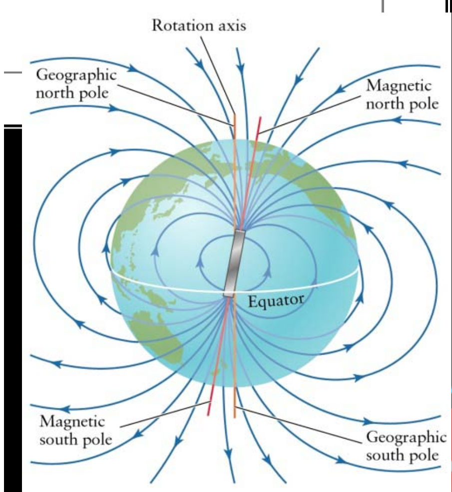

Outline

- Definition of the upper and the lower atmosphere
- Upper Atmosphere (Ionosphere): TEC derivation, advantage, and example application)
- Lower Atmosphere (Troposphere): PWV derivation, example data, Applications
- Some Notes

Definition

Definition of Upper and Lower Atmospheres

Atmospheric layer

- Scientists have defined of both terms in various ways. In the context of meteorologists, the "lower atmosphere" may be described as extending from the planetary surface (the troposphere) to the lower stratosphere where the daily weather evolves.

- Height effective ~ 40 km from sea level.

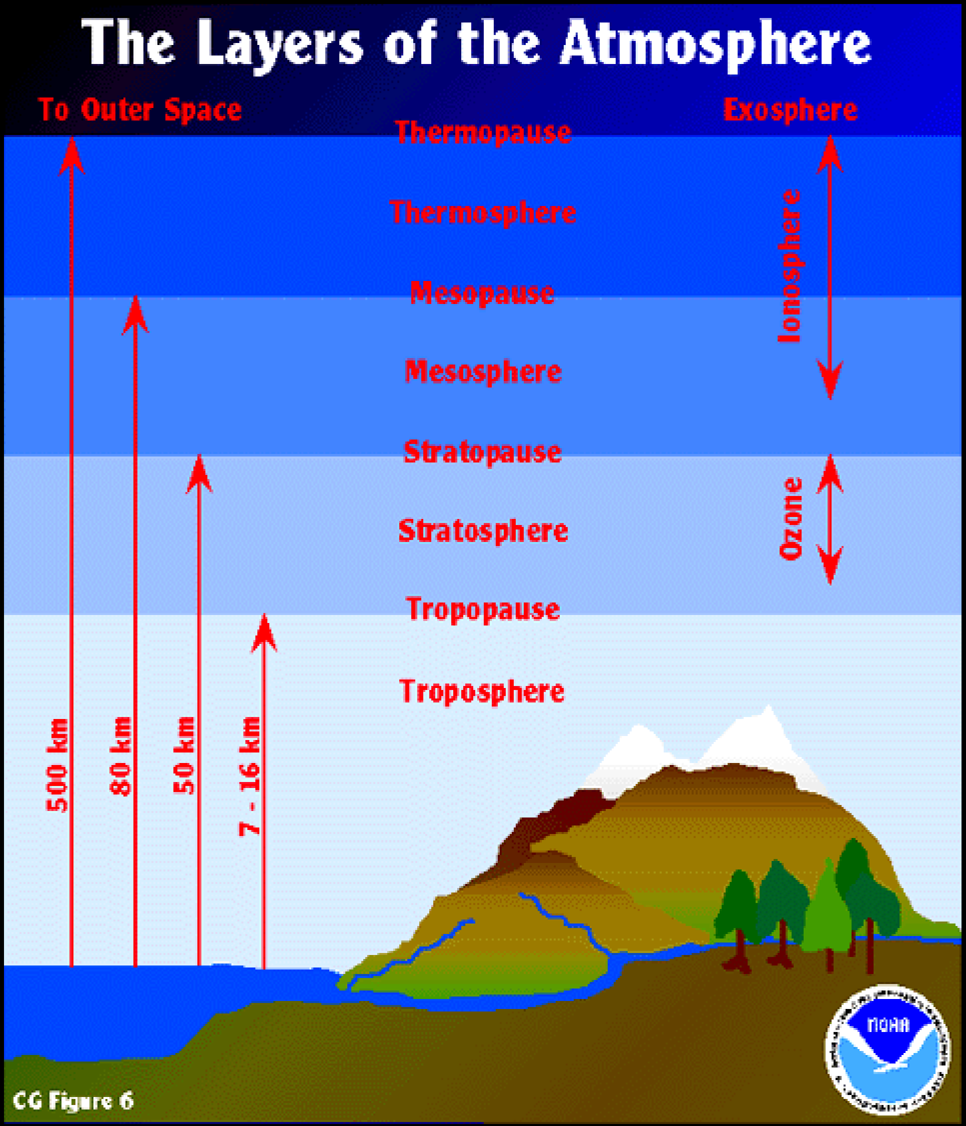

http://www.esrl.noaa.gov/gmd/education/lesson_plans/

- For the "upper atmosphere", it is referred to the entire region above the troposphere includes the mesosphere, the ionosphere and the thermosphere that identified by temperature structure, density, composition and the degree of ionization.

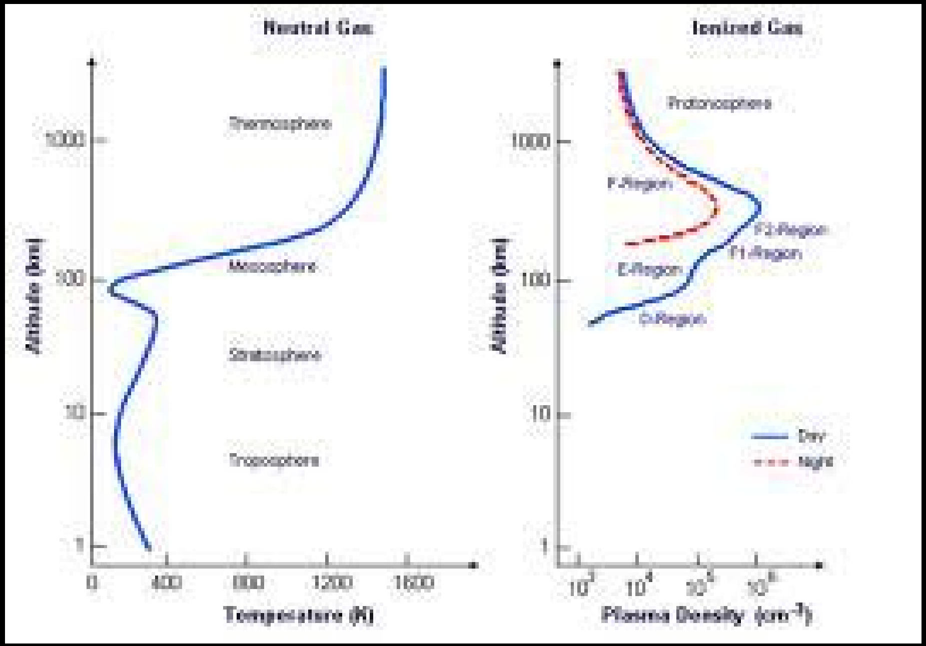

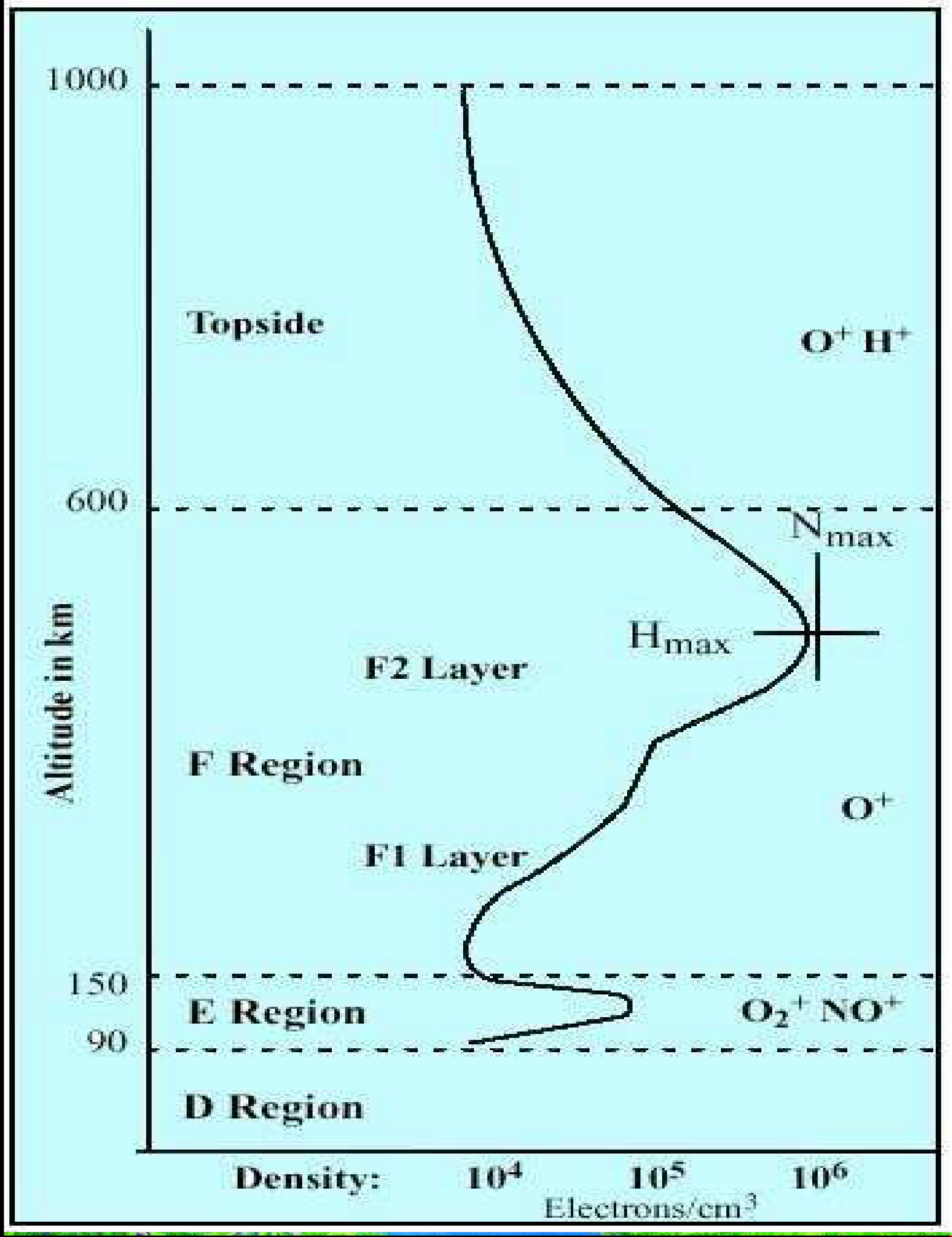

http://utd500.utdallas.edu/ionosphere.htm

- When we looking on the radio waves such as GPS signals propagated through the atmosphere, the atmosphere can be divided into two division; the neutral atmosphere and the ionosphere.

- The neutral atmosphere layer consists of three temperature-delineated regions: the troposphere, the stratosphere and part of the mesosphere. It is often simply referred as the troposphere because in radio wave propagation, the troposphere effects dominate.

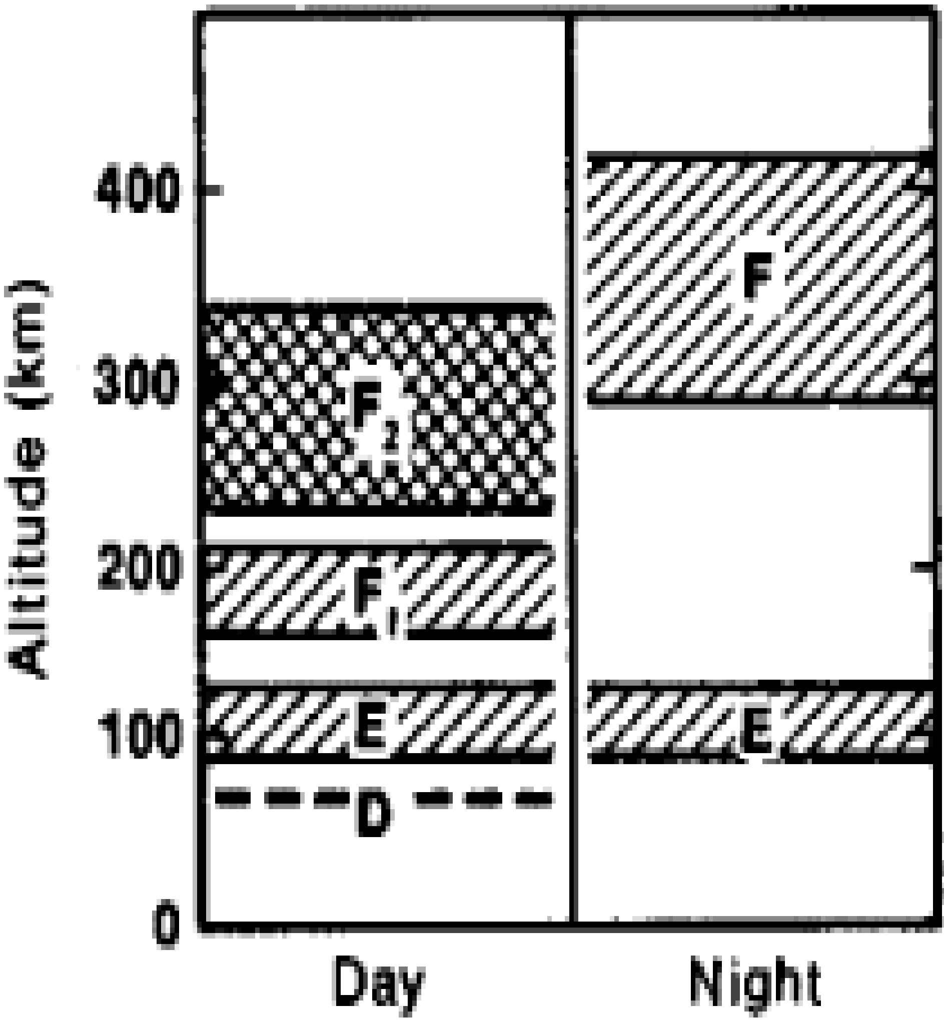

Table 1
Layers of the Ionosphere

Layer	Approximate Elevation	Importance	When Present
F	140 km - 400 km	Main "reflection" region	Always - stronger during daytime
E	90 km - 140 km	Lower frequency "reflection" region	Always - but very weak at night
D	50 km - 90 km	Main absorption region	Daytime only

"Outside of the Earth's atmosphere"

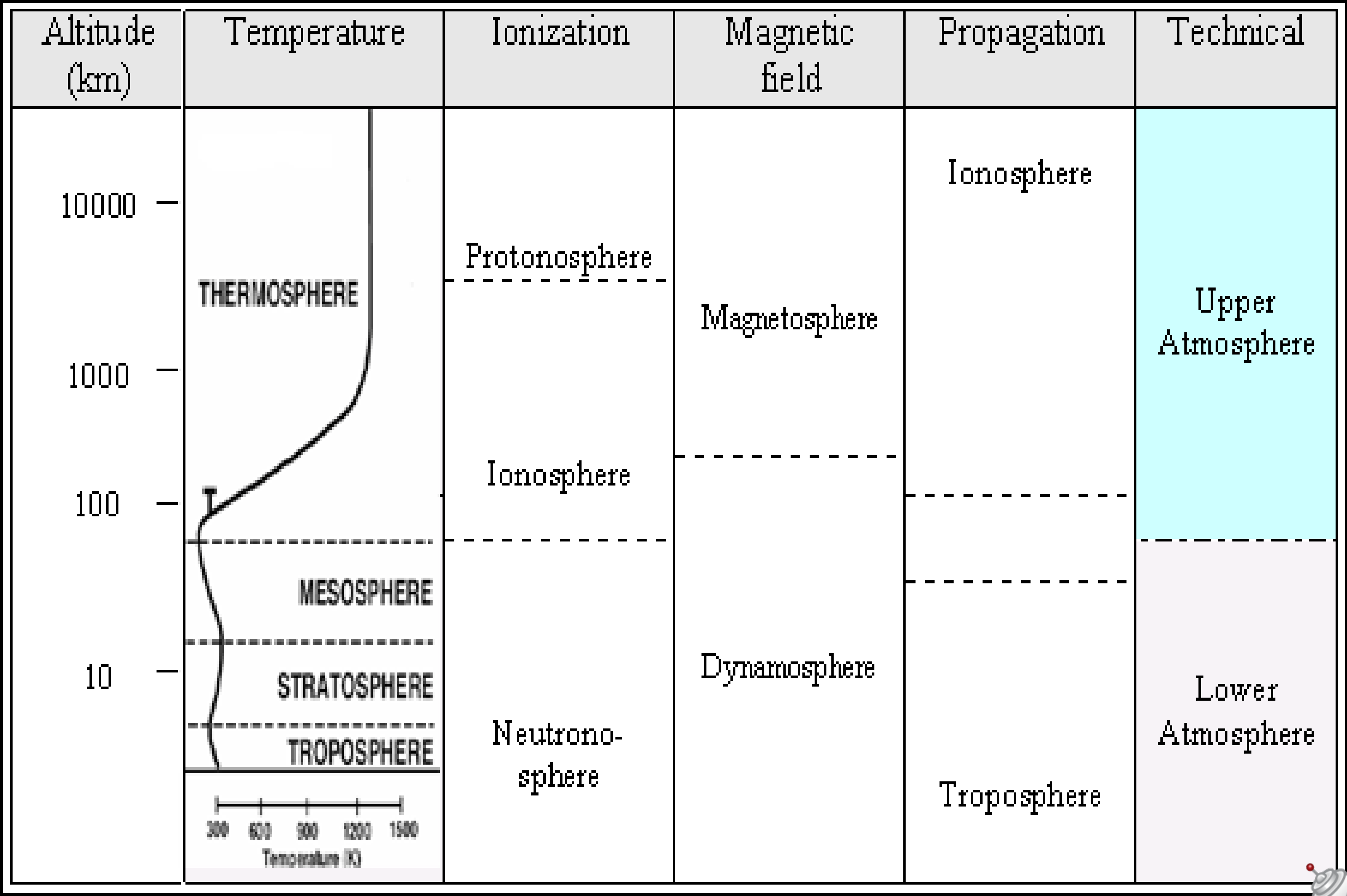

Source: Seeber (1993)

Upper-Lower from GPS Perspective

Wave propagation: the delay

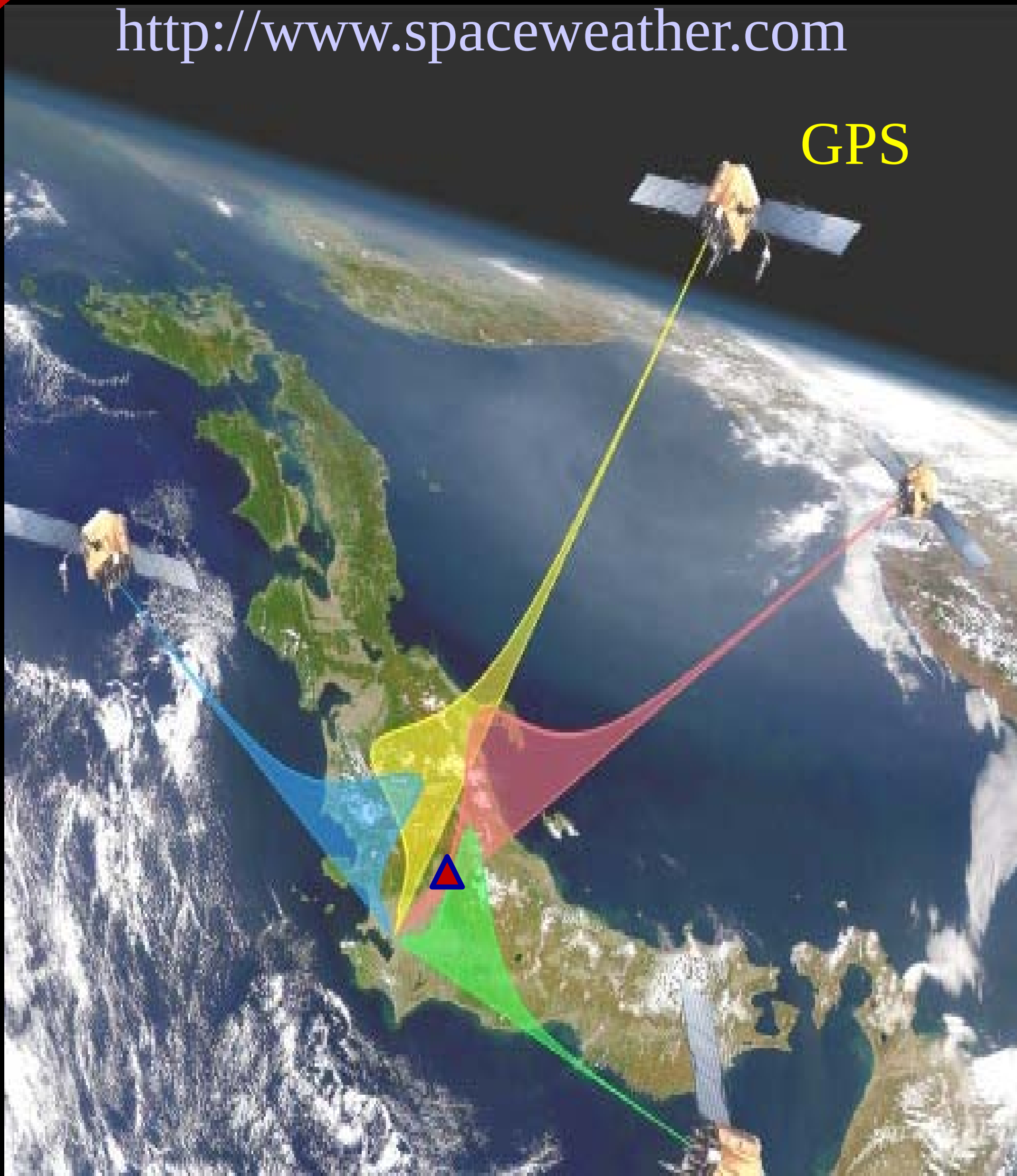

The greatest impact on GPS positional accuracy:

– **Ionosphere δ_{iono}**

– **Troposphere δ_{tropo}**

- By exploiting the delay between GPS and receiver, we are able to extract the total electron content and vertical column of water vapor from GPS measurements.

$$\Delta S = \int_{SV}^{user} N_e \, ds$$

Ionosphere (Upper) – Troposphere (Lower)

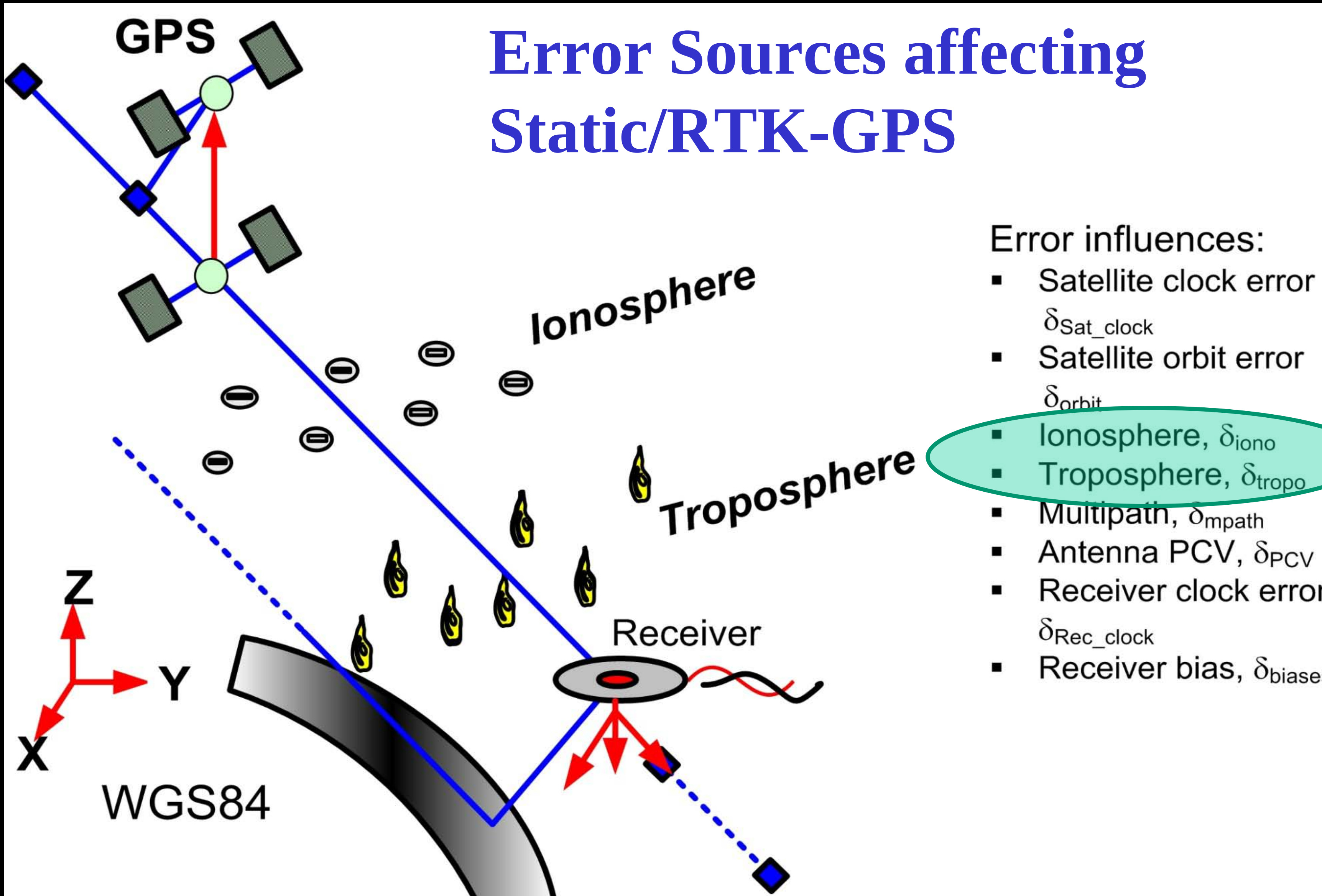

Skyplot for 30 Nov 2007

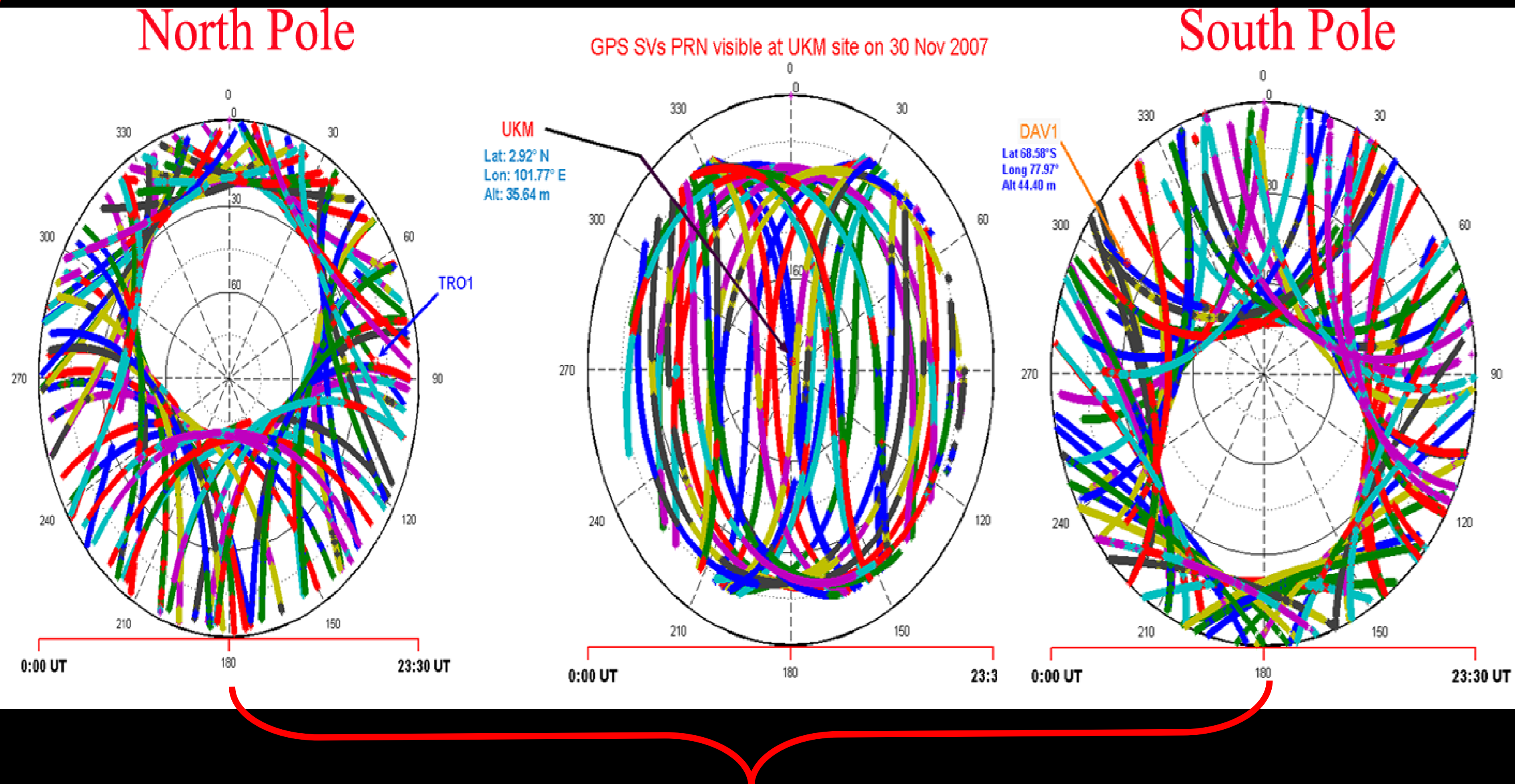

Sky view between North and South Poles are opposite responses

Example TEC Results

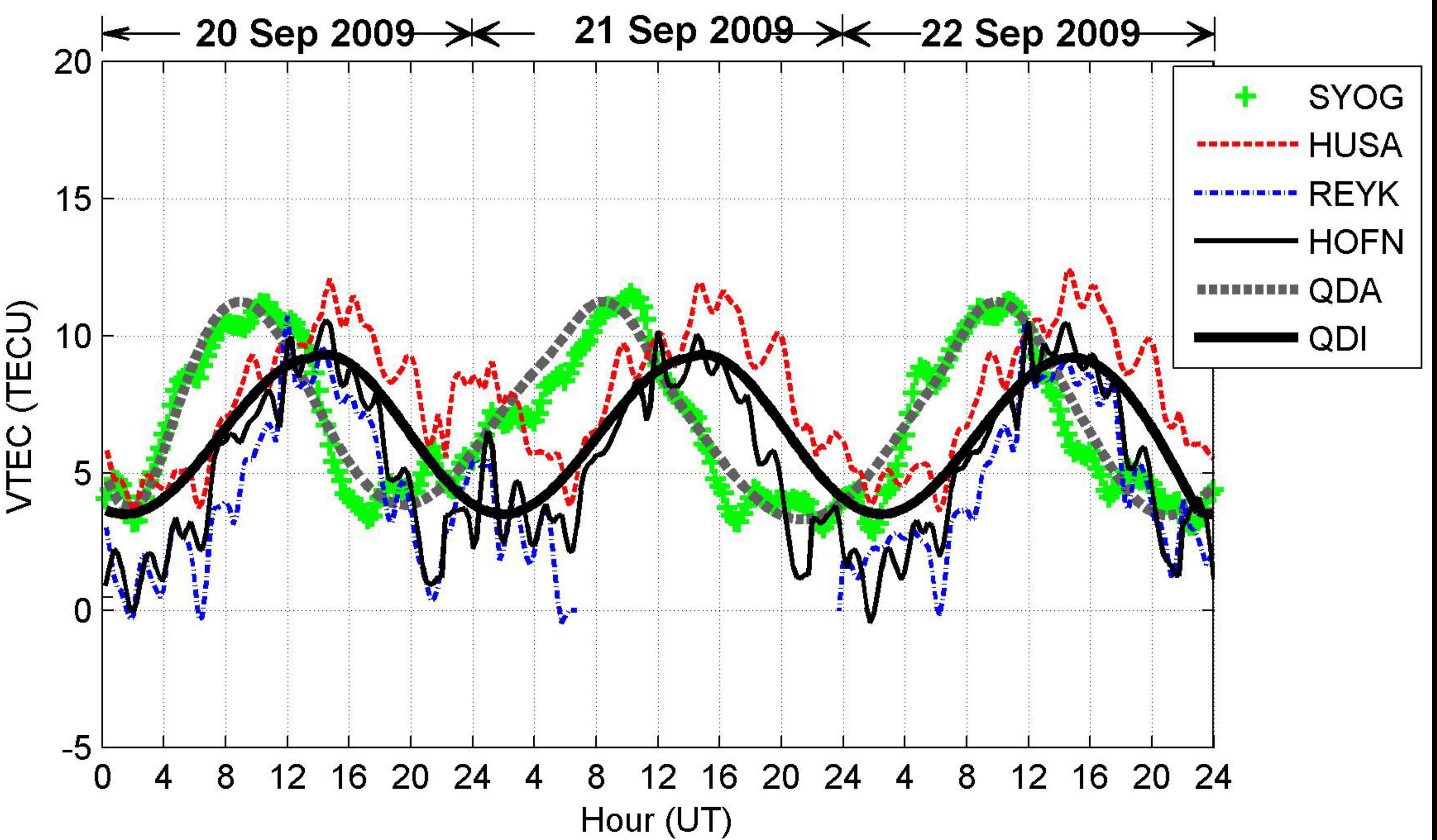

Submitted to JGR-Space Physics (2012)

TEC for selected stations in Antarctica (2007)

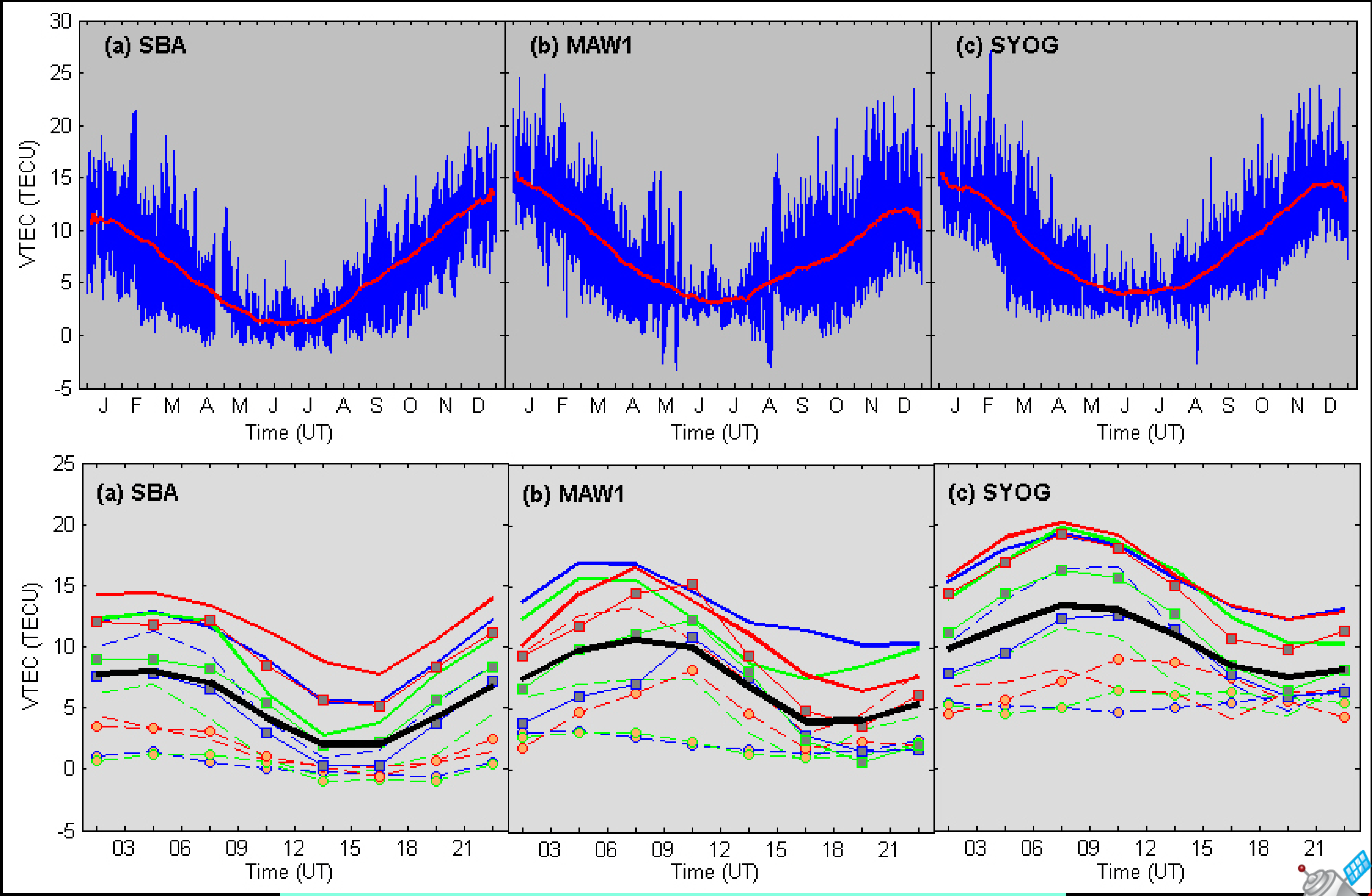

Presented at SCAR 2008

Some Notes

TEC Data Applications:

- Improving positioning accuracy in production of GPS antenna
- Description the quantity for the ionosphere of the Earth
    - ➢ Satellite navigation system
    - ➢ Telecommunication system
- Space weather monitoring and forecasting
- Space weather climatology
- Teleconnections between the ionospheric regions
- Correction factors for GPS users to enhance the accuracy of satellite measurements
- Earthquake and tsunami prediction
- Etc.

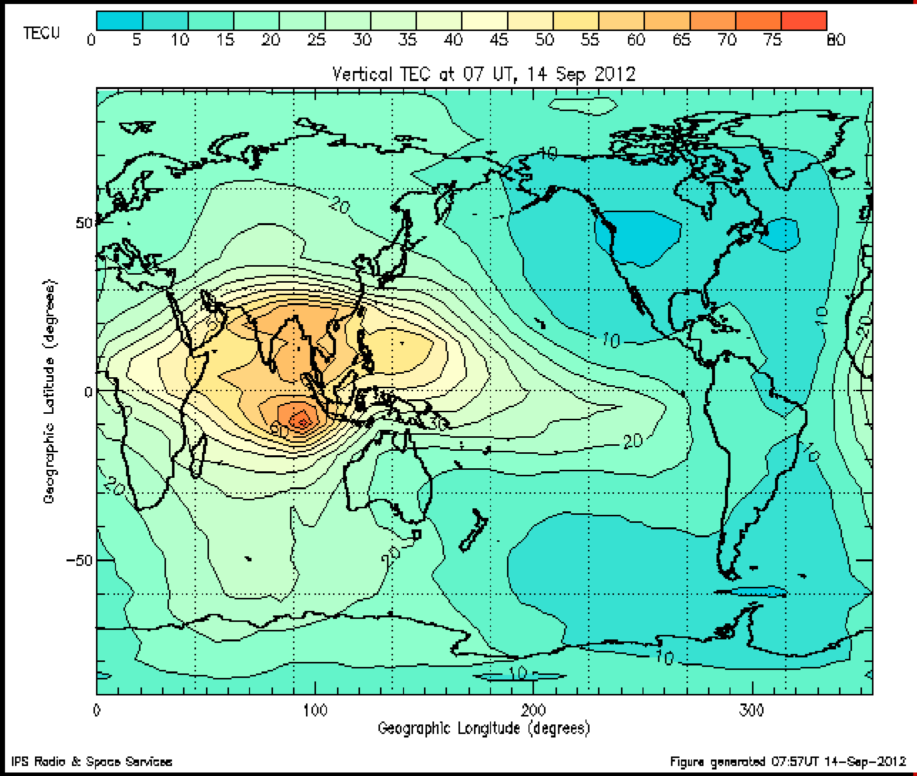

http://www.ips.gov.au/Satellite/2/2

Part 1:

Computing the Total Electron Content (TEC) Using GPS Measurements

GPS TEC

- Currently, several models for accurate TEC estimation to be apply for GPS precise positioning applications has been conducted (Coco et al., 1991; Wanninger, 1993; Klobuchar, 1996 ; Warnant, 1997; Otsuka et al., 2002; Chen et al., 2004; Brunini et al., 2005; Arikan et al., 2008).
- In this work, the TEC computation from GPS observables on *simple (ideal) model* and with *considering instrumental bias* like receiver differential bias, receiver offset, differential code biases (DCBs) or inter-frequency bias (IFB) will be highlighted.

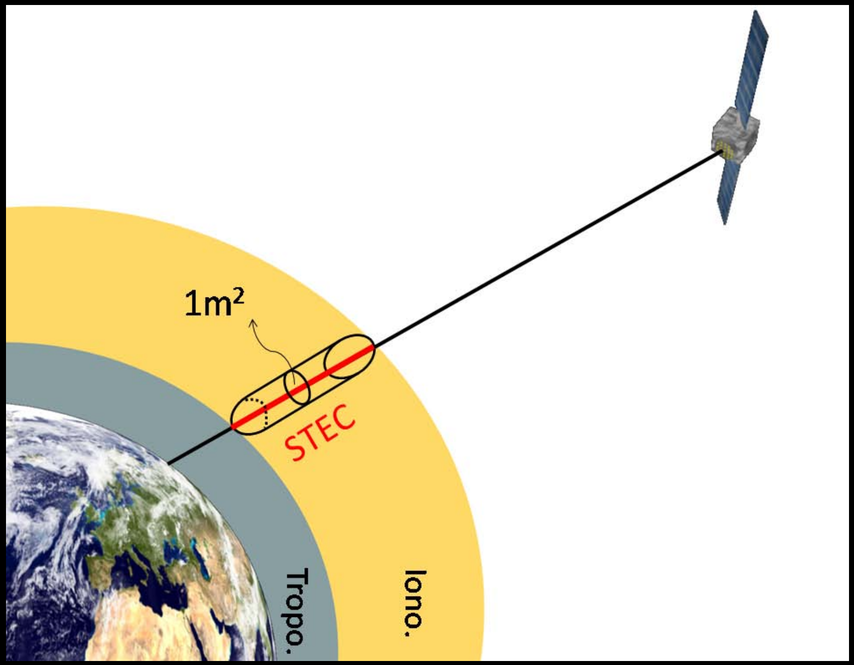

http://gnss.be/

- Many TEC estimation techniques in the literature use the Single Layer Ionosphere Model (SLIM) such as Lanyi and Roth (1988), Schaer (1999), Otsuka et al. (2002), and Arikan et al. (2003).
- I n SLIM model, ionosphere is assumed to be a thin, spherical shell of constant ionospheric height. This height generally corresponds to the height of maximum ionization density.
- SLIM model enables a conversion between slant TEC (STEC) and vertical TEC (VTEC).
- In literature , ionospheric heights from 300 km to 450 km have been used due to varying height of maximum ionization density (Komjathy, 1997) .

- TEC is defined as the line integral of electron density along a raypath L or as a measure of the total number of electrons along a path of the radio wave (Budden, 1985)

$$TEC = \int_S N_e(s)\,ds \qquad (1)$$

- with **refractivity** is defined as $N = 10^6(n - 1)$

$$n = 1 - \frac{40.3}{f^2} N$$

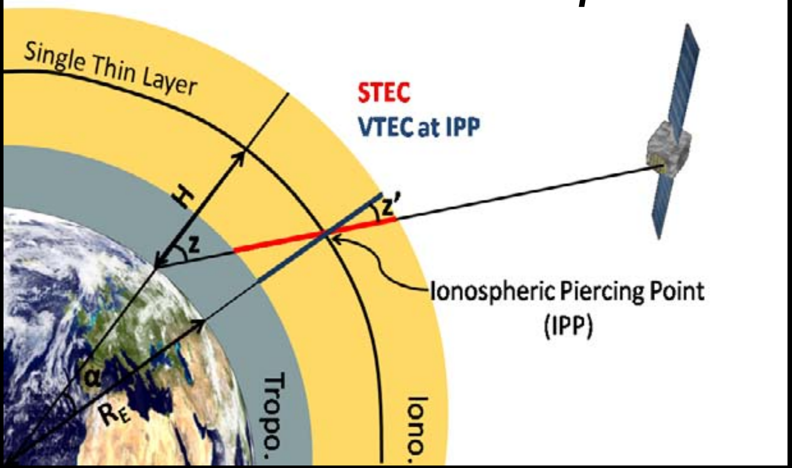

- The propagation velocity of the ionosphere at GPS frequencies (Hofmann-Wellenhof, 2001) for phase and group velocity, can be expressed as

$$v_p = \frac{c}{n_p},\ v_g = \frac{c}{n_g} = v_p - \lambda \frac{dv_p}{d\lambda} \qquad (2)$$

- Differentiation of the phase velocity with respect to λ

$$\frac{dv_p}{d\lambda} = -\frac{c}{n_p^2}\frac{dn_p}{d\lambda} \qquad (3)$$

- The refractive index (n) of the ionosphere at GPS frequencies for phase and group, can be expressed as

$$n_g = n_p + f\frac{dn_{ph}}{df} \qquad (4)$$

$$n_p = 1 + \frac{A}{f^2} + \frac{B}{f^3} + \frac{C}{f^4} + \ldots \cong 1 + \frac{A}{f^2} \qquad (5)$$

$$dn_p = -\frac{2A}{f^3}df \;\Rightarrow\; n_g = 1 - \frac{A}{f^2} \qquad (6)$$

- The STEC at the point of intersection of the GPS ray path with the ionospheric shell, can be determined using range error (e.g., Yizengav, yesterday)

$$STEC = \int_0^s N dr = \left(\frac{f_2^2}{f_1^2 - f_2^2}\right)\frac{2f_1^2}{K}\Delta P_{1,2} \qquad (7)$$

- STEC can also be computed using differential phase advance

$$STEC = \int_0^s N dr = \left(\frac{f_2^2}{f_1^2 - f_2^2}\right)\frac{2f_1^2}{K}\Delta L_{1,2} \qquad (8)$$

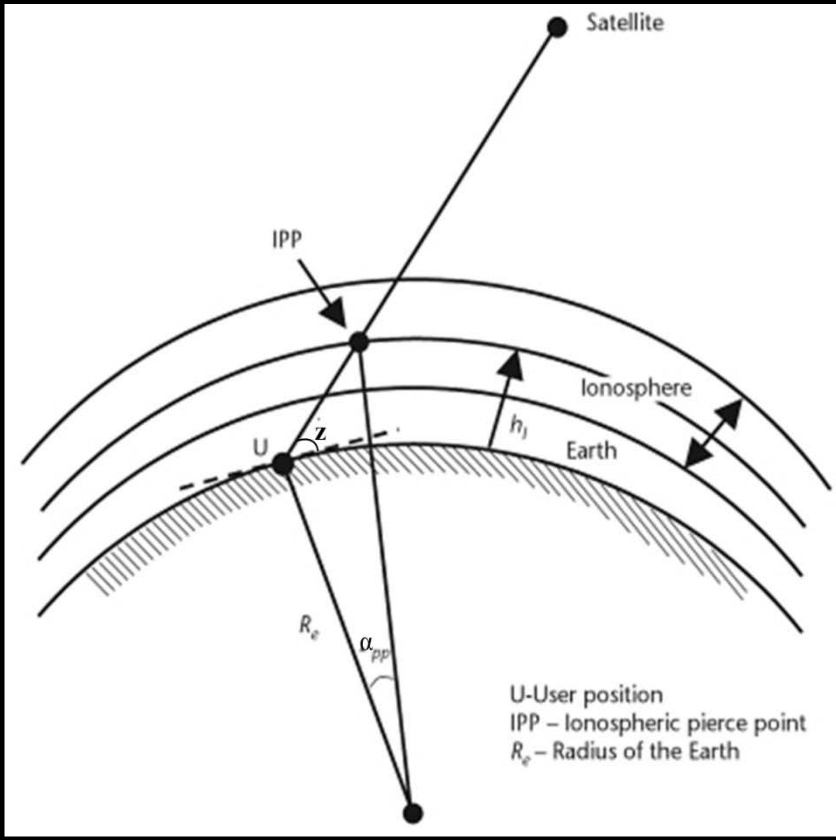

- In both cases, the STEC can be converted to VTEC at IPP as follow:

$$VTEC = STEC \cos z' \qquad (9)$$

$$\sin^2 z + \cos^2 z = 1, \; and \;\; z = 90^0 - \alpha$$

- and an abliguity factor or mapping function:

$$\sin z' = \frac{R_E}{R_E + h_m} \sin z \qquad (10)$$

$$\cos z' = \left(1 - \frac{R_E^2 \cos^2 \alpha}{(R_E + h_m)^2}\right)^{1/2}$$

RINEX (*.obs): An example

```
     2.11           OBSERVATION DATA    G (GPS)             RINEX VERSION / TYPE
teqc  2012Jun6      gpsops              20120719 00:06:00UTCPGM / RUN BY / DATE
Linux 2.4.21-27.ELsmp|Opteron|gcc -static|Linux x86_64|=+    COMMENT
BIT 2 OF LLI FLAGS DATA COLLECTED UNDER A/S CONDITION        COMMENT
MCM4                                                        MARKER NAME
66001M003                                                   MARKER NUMBER
GGN                 JPL                                     OBSERVER / AGENCY
ZR520021808         ASHTECH UZ-12       CQ00                REC # / TYPE / VERS
363                 AOAD/M_T        JPLA                    ANT # / TYPE
 -1311703.1720   310814.9820 -6213255.1600                  APPROX POSITION XYZ
        0.0814        0.0000        0.0000                  ANTENNA: DELTA H/E/N
     1     1                                                WAVELENGTH FACT L1/2
     5    L1    L2    P1    P2    C1                        # / TYPES OF OBSERV
    30.0000                                                 INTERVAL
                                                            COMMENT
Forced Modulo Decimation to 30 seconds                      COMMENT
 SNR is mapped to RINEX snr flag value [0-9]                COMMENT
  L1 & L2: min(max(int(snr_dBHz/6), 0), 9)                  COMMENT
pseudorange smoothing corrections not applied               COMMENT
  2012     7    18     0     0    0.0000000     GPS         TIME OF FIRST OBS
                                                            END OF HEADER
 12  7 18  0  0  0.0000000  0 12G15G29G07G18G16G30G03G26G08G06G21G05
  -5391071.56347  -4179509.24647  23940202.5944   23940205.4374   23940202.687
  -5892260.98447  -4536889.82347  24532989.0584   24532992.9604   24532988.532
 -10347049.67548  -8053040.59247  22669558.1124   22669559.6984   22669557.535
  -3134453.34147  -2425842.28846  23612919.3534   23612922.2284   23612918.859
 -14661264.42848 -11117287.30147  22568001.0174   22568003.5114   22568000.263
  -7631781.05947  -5888442.88046  24528124.7934   24528128.1564   24528126.597
  -8492795.01647  -6598234.42147  23463584.0494   23463587.5444   23463584.486
 -13717288.98348 -10674980.23147  22679192.8814   22679195.9244   22679192.118
 -11751529.17648  -9090416.60147  22765380.6074   22765384.8114   22765381.581
 -18837440.99148 -14608315.66547  22389910.4594   22389913.1204   22389910.712
 -23338070.53349 -18090676.01548  20683955.2054   20683957.4504   20683955.151
 -15398245.53648 -11983252.26347  22628998.1034   22629000.9294   22628997.671
 12  7 18  0  0 30.0000000  0 12G15G29G07G18G16G30G03G26G08G06G21G05
  -5496040.57647  -4261303.22947  23920228.0474   23920229.8184   23920226.722
  -5773814.08547  -4444593.74846  24555527.9004   24555532.3824   24555527.357
 -10317577.88948  -8030075.56047  22675165.9544   22675168.2494   22675164.931
  -3251068.95647  -2516711.61946  23590727.5154   23590729.9484   23590727.215
 -14610405.74748 -11077657.20147  22577679.4104   22577681.2804   22577679.454
  -7537361.42647  -5814869.13946  24546093.0654   24546093.3784   24546093.608
  -8566572.94147  -6655723.71447  23449545.8374   23449549.0324   23449545.388
 -13768117.32348 -10714586.72047  22669520.3614   22669523.6644   22669520.000
 -11807856.72948  -9134308.20447  22754661.3534   22754664.8464   22754661.216
 -18902672.38748 -14659145.31147  22377497.1474   22377500.8194   22377496.966
 -23347488.99049 -18098015.08048  20682162.7664   20682165.2044   20682162.827
 -15315385.63848 -11918686.12347  22644766.5954   22644768.1064   22644765.327
 12  7 18  0  1  0.0000000  0 12G15G29G07G18G16G30G03G26G08G06G21G05
  -5600756.88347  -4342900.32147  23900300.9124   23900302.9824   23900301.523
  -5655231.20347  -4352191.61746  24578094.6814   24578095.0774   24578093.726
 -10287461.15348  -8006607.99047  22680896.9554   22680899.4914   22680895.997
```

Header

Data

GPS TEC with instrumental biases

- The standard model for pseudorange recording for two frequencies f_1 and f_2 are as follows (Leick, 2004):

$$P_{1,r}^{s} = p_r^s + c\left(\delta t_r - \delta t^s\right) - d_{trop}^{s} + d_{ion1}^{s} + c\left(\varepsilon_1^s + \varepsilon_{1,r}\right) \quad (11)$$

$$P_{2,r}^{s} = p_r^s + c\underbrace{\left(\delta t_r - \delta t^s\right)}_{\text{Clock errors}} - d_{trop}^{s} + d_{ion2}^{s} + c\underbrace{\left(\varepsilon_2^s + \varepsilon_{2,r}\right)}_{\text{Biases}} \quad (12)$$

- The difference between (11) and (12) is called the geometry free linear combination of pseudorange because of the actual range p is eliminated as

$$\begin{aligned} P_{4,r}^{s} &= P_{2,r}^{s} - P_{1,r}^{s} \\ &= d_{ion2}^{s} - d_{trop}^{s} + c\underbrace{\left(\varepsilon_2^s - \varepsilon_1^s\right)}_{DCB^s} + c\underbrace{\left(\varepsilon_{2,r} - \varepsilon_{1,r}\right)}_{DCB_r} \end{aligned} \quad (13)$$

- Similar equations can be written for phase delay observations (Leick, 2004):

$$L_{1,r}^{s} = \lambda_1 \Phi_{1,r}^{s} = p_r^s + c\left(\delta t_r - \delta t^s\right) + \lambda_1 \Phi_{ion1,r}^{s} + \lambda_1 \Phi_{trop,r}^{s} - c\left(\varepsilon_1^s + \varepsilon_{1,r}\right) + \lambda_1 N_1^s \quad (14)$$

$$L_{2,r}^{s} = \lambda_2 \Phi_{2,r}^{s} = p_r^s + c\left(\delta t_r - \delta t^s\right) + \lambda_2 \Phi_{ion2,r}^{s} + \lambda_2 \Phi_{trop,r}^{s} - c\left(\varepsilon_2^s + \varepsilon_{2,r}\right) + \lambda_2 N_2^s \quad (15)$$

N_1^s and N_2^s, denote the initial phase ambiguity of f_1 and f_2

- The difference between (14) and (15) is called the geometry free linear combinations of phase delay and is given as

$$L_{4,r}^{s} = \lambda_1 \Phi_{1,r}^{s} - \lambda_2 \Phi_{2,r}^{s} = \lambda_1 \Phi_{ion1,r}^{s} - \lambda_2 \Phi_{ion2,r}^{s} + c\left(DCB^s\right) + c\left(DCB_r\right) + \Delta N^s \quad (16)$$

$$\Delta N^s = \lambda_1 N_1^s - \lambda_2 N_2^s$$

- Using the approximation given by Liao (2000) and Leick (2004):

$$d_{ion,r}^{s} = -\Phi_{ion,r}^{s} \frac{c}{f} \approx A \frac{STEC_r^s}{f^2}, \quad A = 40.3\, m^3 / s^2 \quad (17)$$

- Using equation (17) in equations (13) and (16), the expressions for the geometry free combinations are obtained as follows (Leick, 2004; Komjathy, 1997; Nayir, 2007):

$$P_{4,r}^{s} = A\left(\frac{f_1^2 - f_2^2}{f_1^2 f_2^2}\right) STEC_r^s - c\left(DCB^s - DCB_r\right) \quad (18)$$

$$L_{4,r}^{s} = A\left(\frac{f_1^2 - f_2^2}{f_1^2 f_2^2}\right) STEC_r^s - c\left(DCB^s - DCB_r\right) + \Delta N^s \quad (19)$$

- STEC values for each satellite and receiver pair can be obtained from (19) as

$$STEC_r^s(n) = \frac{1}{A}\left(\frac{f_1^2 f_2^2}{f_1^2 - f_2^2}\right)\left[P_{4,r}^s(n) + c\left(DCB^s - DCB_r\right)\right] \quad (20)$$

n is sample time ($1 \le n \le N$), for 24h with data recorded every 30s, N = 2880.

How to solve ΔN^s or STEC computed using phase delay?

- One method can be employed is leveling or fitting of L_4 to P_4 by defining a baseline for each connected arc of phase measurements (Lanyi and Roth, 1988; Otsuka et al., 2002):

$$B^s = \frac{1}{N_{me}} \sum_{n_{me}=1}^{N_{me}} \left(P^s_{4,r}(n_{me}) - L^s_{4,r}(n_{me}) \right) \quad (21)$$

where N_{me} is time duration of total samples, and n_{me} is the time index of the samples in the connected phase arc.

- The STEC now can be expressed as follow:

$$STEC^s_r(n) = \frac{1}{A} \left(\frac{f_1^2 f_2^2}{f_1^2 - f_2^2} \right) \left[B^s + L^s_{4,r}(n) + c\left(DCB^s + DCB_r \right) \right] \quad (22)$$

Now STEC can be computed using (20) or (22). The STEC can be converted to VTEC using (9).

- Similar equations can be written for phase delay observations (Leick, 2004):

$$L_{1,r}^{s} = \lambda_1 \Phi_{1,r}^{s} = p_r^s + c\left(\delta t_r - \delta t^s\right) + \lambda_1 \Phi_{ion1,r}^{s} + \lambda_1 \Phi_{trop,r}^{s} - c\left(\varepsilon_1^s + \varepsilon_{1,r}\right) + \lambda_1 N_1^s \quad (14)$$

$$L_{2,r}^{s} = \lambda_2 \Phi_{2,r}^{s} = p_r^s + c\left(\delta t_r - \delta t^s\right) + \lambda_2 \Phi_{ion2,r}^{s} + \lambda_2 \Phi_{trop,r}^{s} - c\left(\varepsilon_2^s + \varepsilon_{2,r}\right) + \lambda_2 N_2^s \quad (15)$$

N_1^s and N_2^s, denote the initial phase ambiguity of f_1 and f_2

- The difference between (14) and (15) is called the geometry free linear combinations of phase delay and is given as

$$L_{4,r}^{s} = \lambda_1 \Phi_{1,r}^{s} - \lambda_2 \Phi_{2,r}^{s} = \lambda_1 \Phi_{ion1,r}^{s} - \lambda_2 \Phi_{ion2,r}^{s} + c\left(DCB^s\right) + c\left(DCB_r\right) + \Delta N^s \quad (16)$$

$$\Delta N^s = \lambda_1 N_1^s - \lambda_2 N_2^s$$

- Using the approximation given by Liao (2000) and Leick (2004):

$$d_{ion,r}^{s} = -\Phi_{ion,r}^{s} \frac{c}{f} \approx A \frac{STEC_r^s}{f^2}, \quad A = 40.3\, m^3 / s^2 \quad (17)$$

Satellite elevation angle

Convert DAT (binary format) to RINEX using TEQC for *.O and *.n

Go through if the GPS data from the internet (e.g. SOPAC)

Convert RINEX to mat/ascii files (s1l1, s1l2, s1c1, s1p2, s1eph, s1epo, s1head, and s1log)

Use the rinex2mat.m with rinex_o.exe and rinex_n.exe

Calculation of GPS receiver position (user)

Position determination of each satellite using Keppler equation

Determination of the elevation angle (θ) based on WGS84 frame

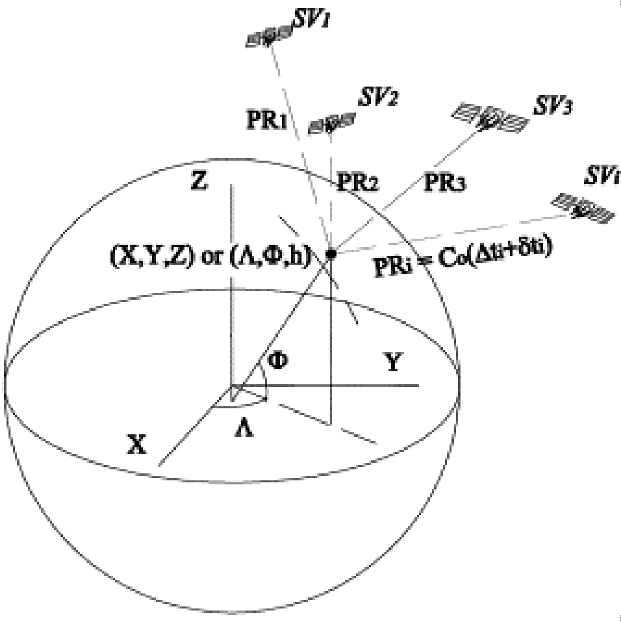

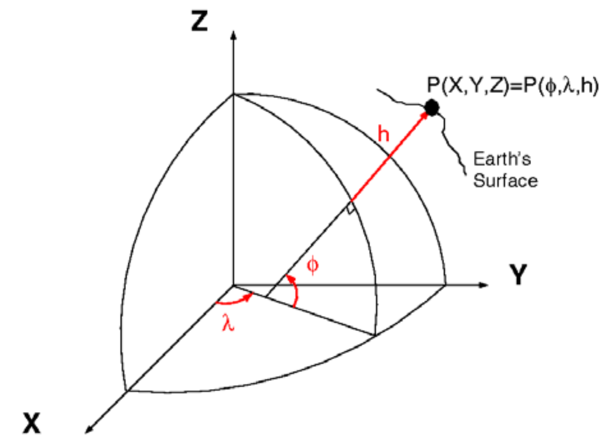

- The formula for calculation elevation angle is given as

$$\theta(x, y, z, t) = \sin^{-1}\left(up \bullet V\right) \qquad (4)$$

with

$$V = [X_k / D(t, nsat); Y_k / D(t, nsat); Z_k / D(t, nsat)]$$

$$D(t, nsat) = \left((X_k - X_r)^2 + (Y_k - Y_r)^2 + (Z_k - Z_r)^2\right)^{\frac{1}{2}} \qquad (5)$$

$$up = \left[X_r / R_r ; Y_r / R_r ; Z_r / R_r\right]$$

$$R_r = \left(X_r^2 + Y_r^2 + Z_r^2\right)^{\frac{1}{2}}$$

where

V is vector position of each satellite at any given time,

up is unit vector at the receiver position,

$D(t, nsat)$ is geometry range ‘topocentric’ between receiver and *n* satellite view at given time *t*.

TEC for selected stations in Antarctic and Arctic

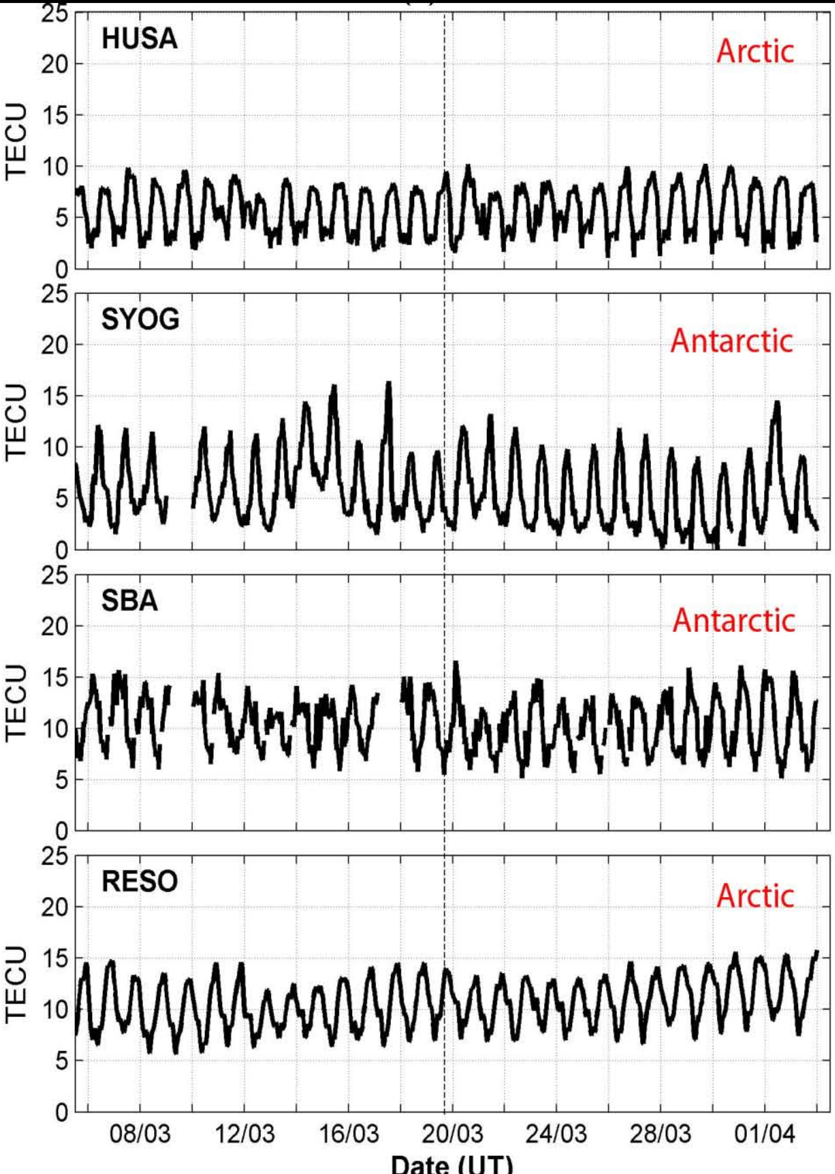

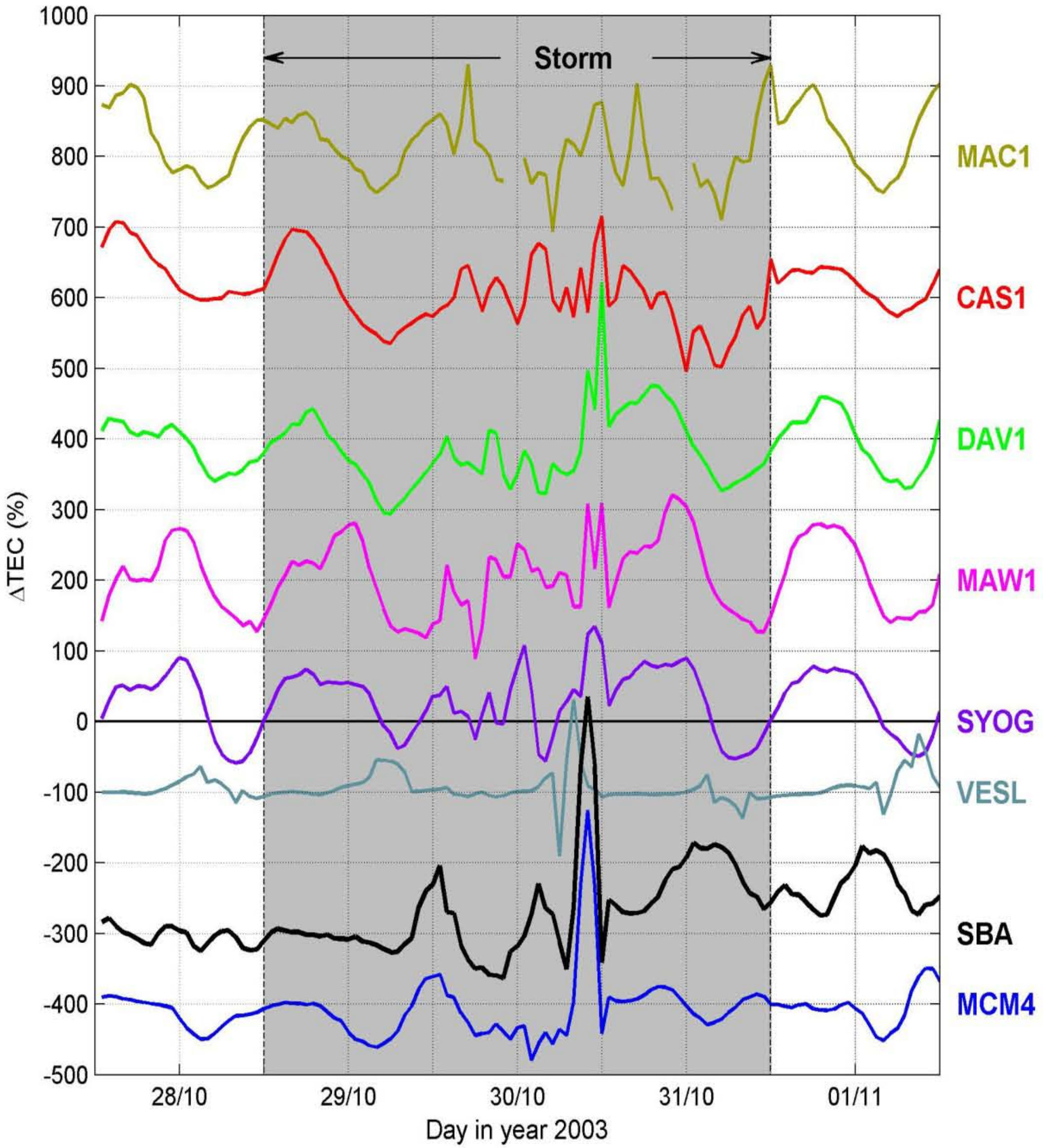

Submitted to IJRS (2012)

DOI: 10.3844/ajassp.2012.894.901

Another TEC for selected stations in Antarctic region

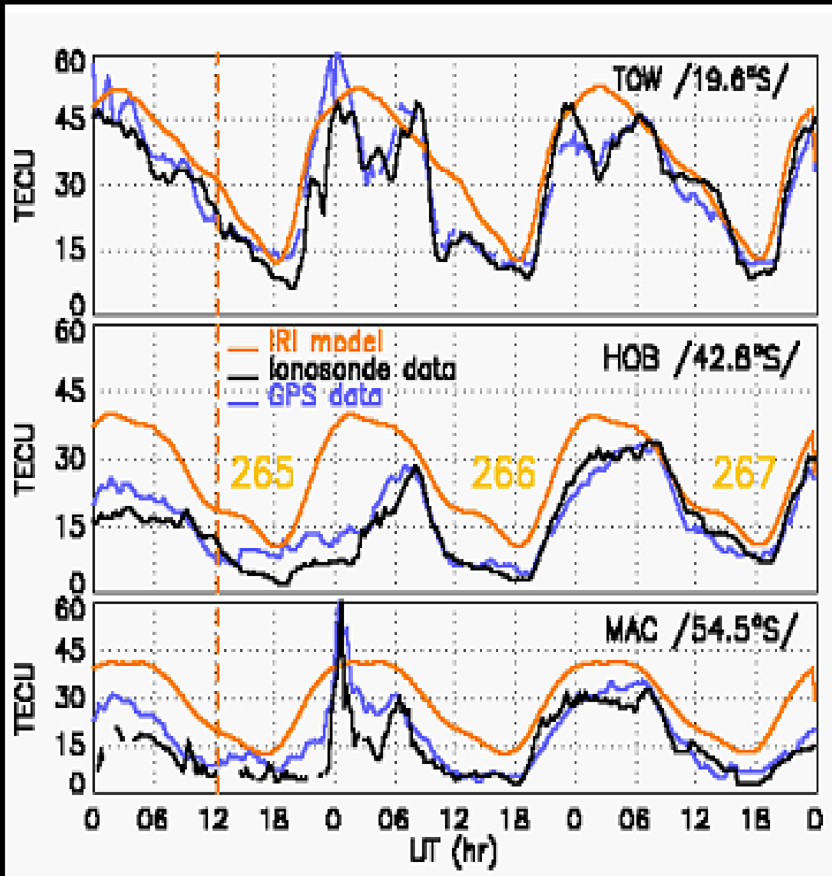

Diurnal TEC variation at derived from GPS, Ionosonde and IRI2000 model

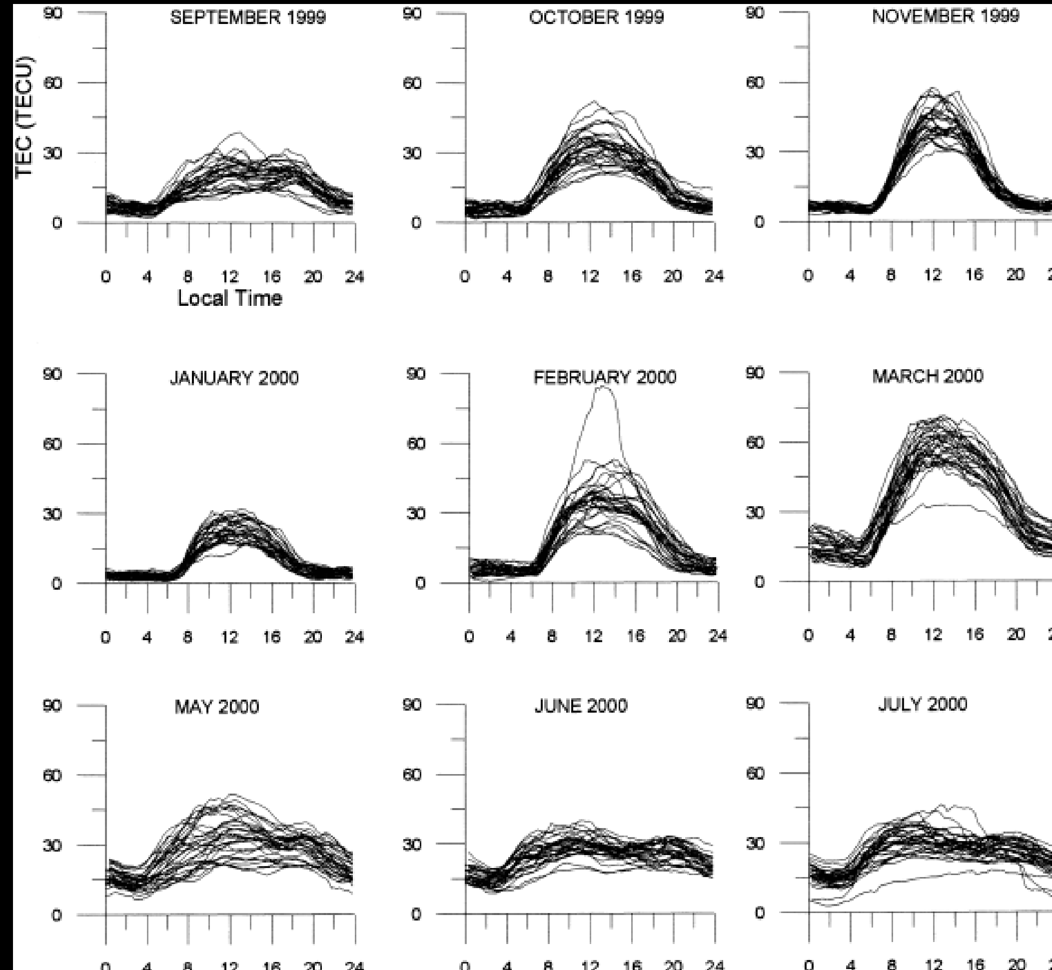

Diurnal TEC variation at Brussels

Yizengav and Essex (2010)

Warnant and Pottiaux (2000)

Real-time Global Map TEC

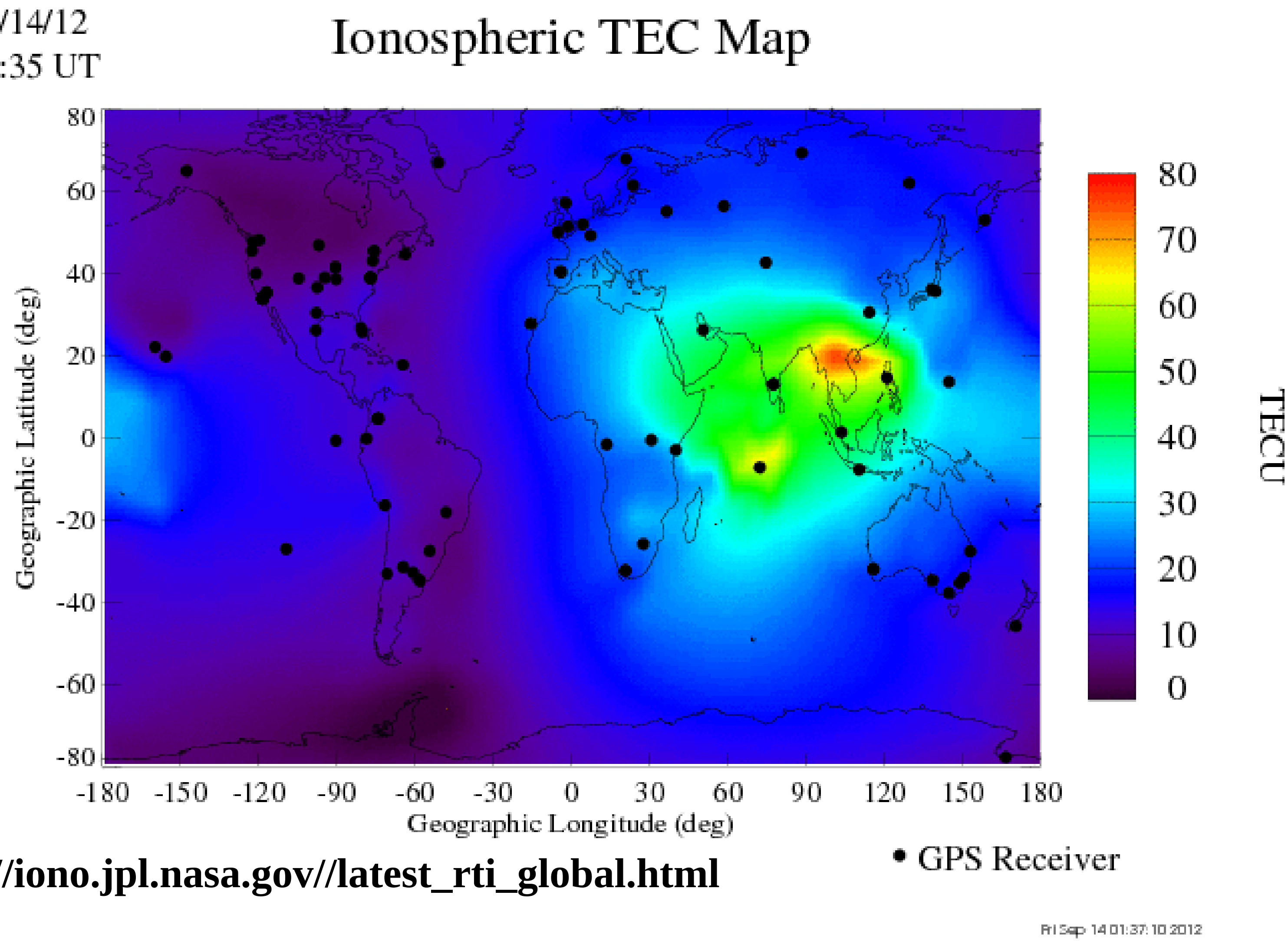

http://iono.jpl.nasa.gov//latest_rti_global.html

TEC between the hemispheres (21/09/2009)

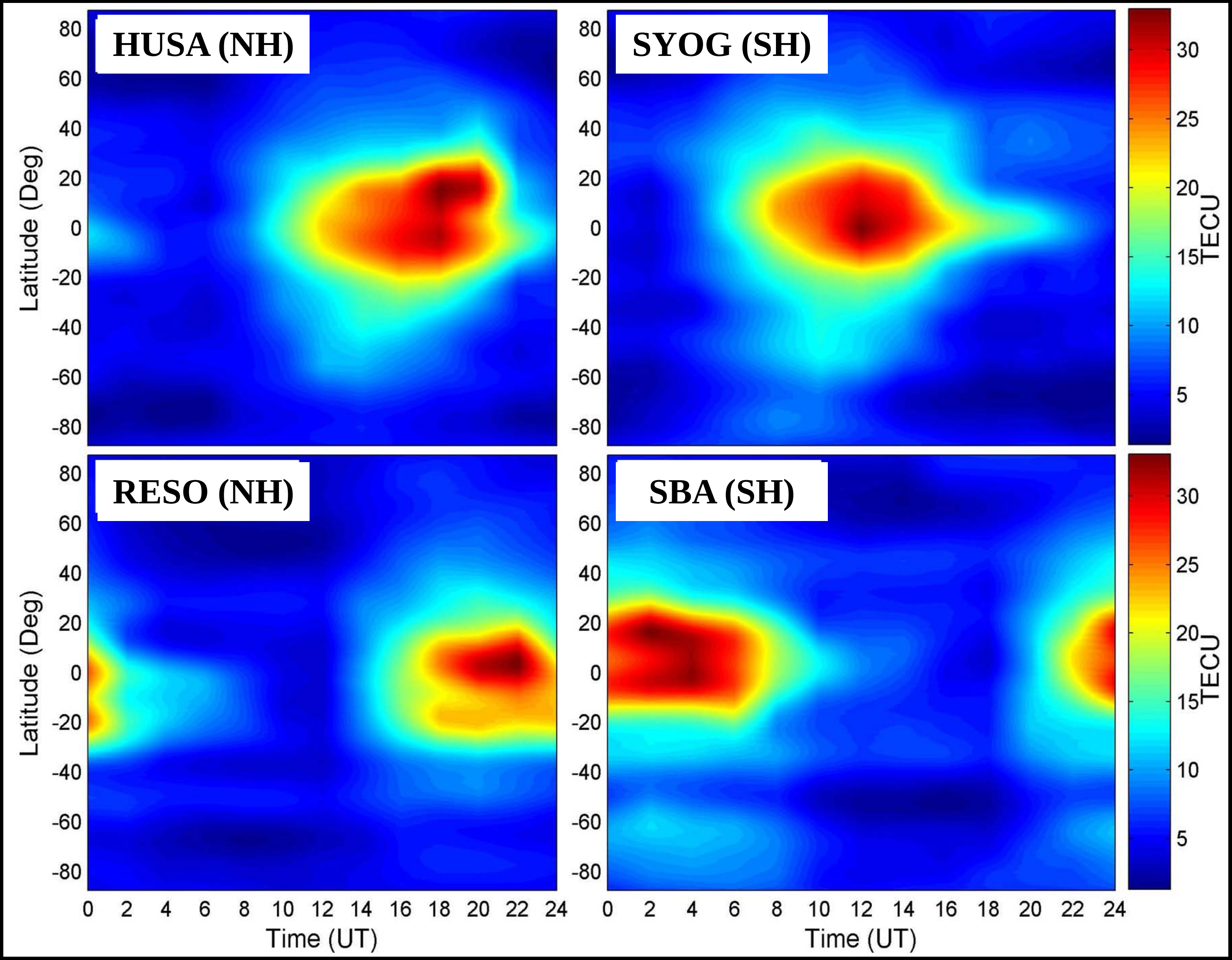

TEC data use for aurora study

GPS TEC variations in Polar Regions

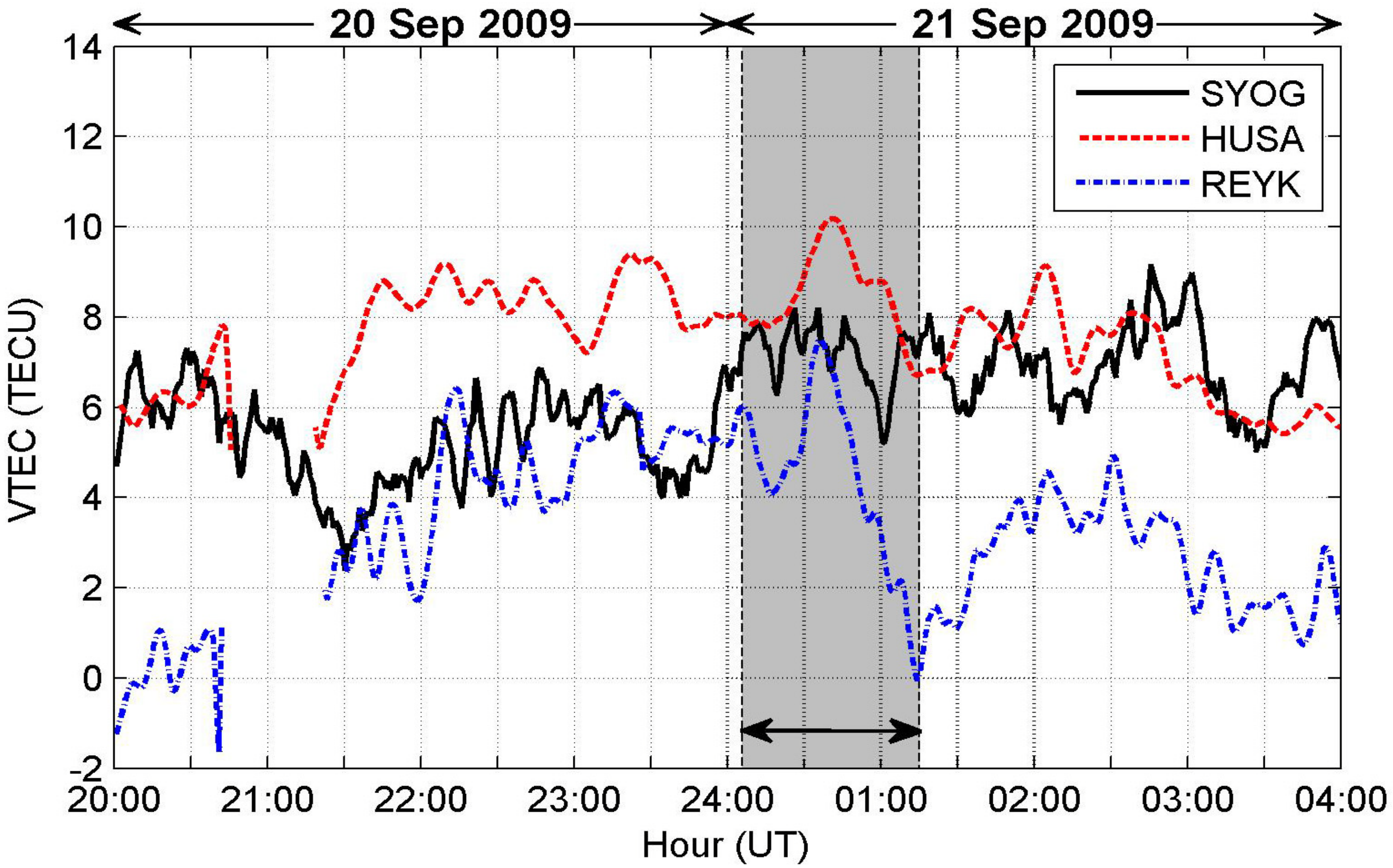

What is aurora?

Auroras are usually observed at night and are commonly visible between 65 to 72 degrees north and south latitudes, which place them in a ring just within the Arctic and Antarctic circles.

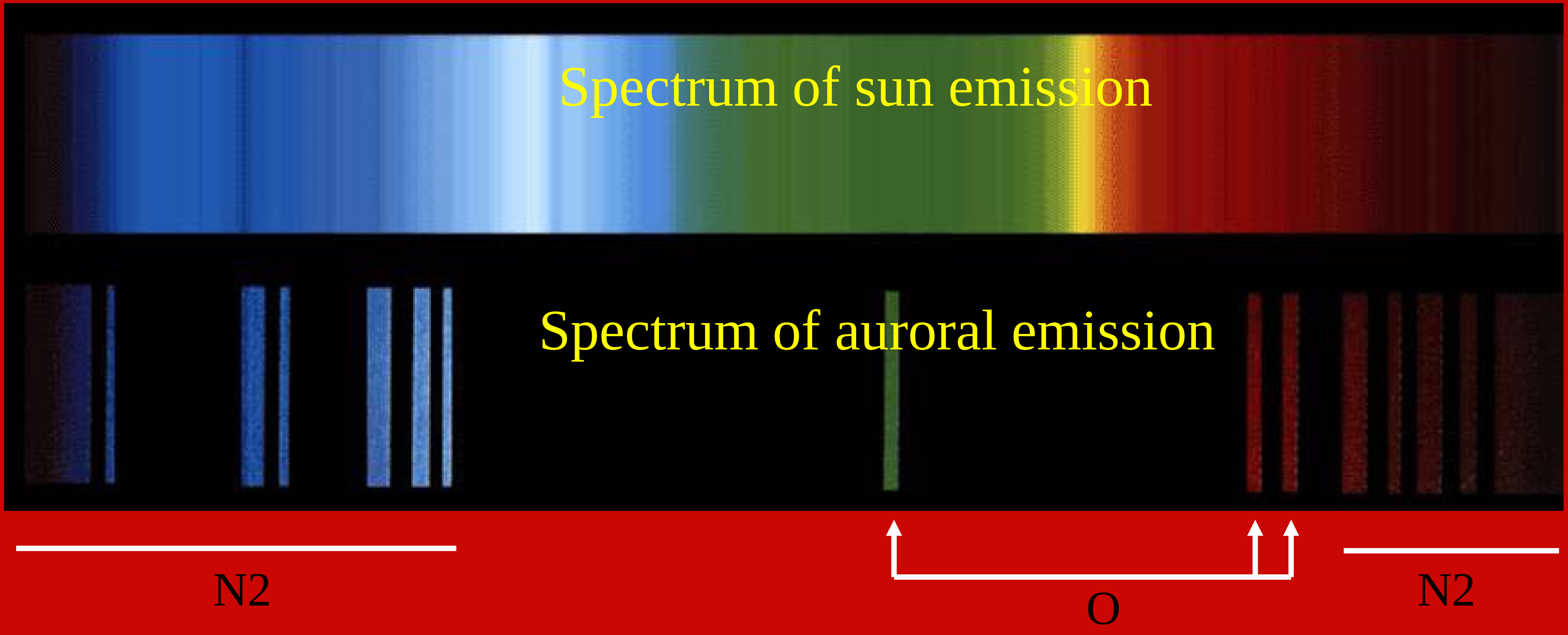

Intermittent spectrum for the aurora (Sato, 2009)

Auroral emission spectrum

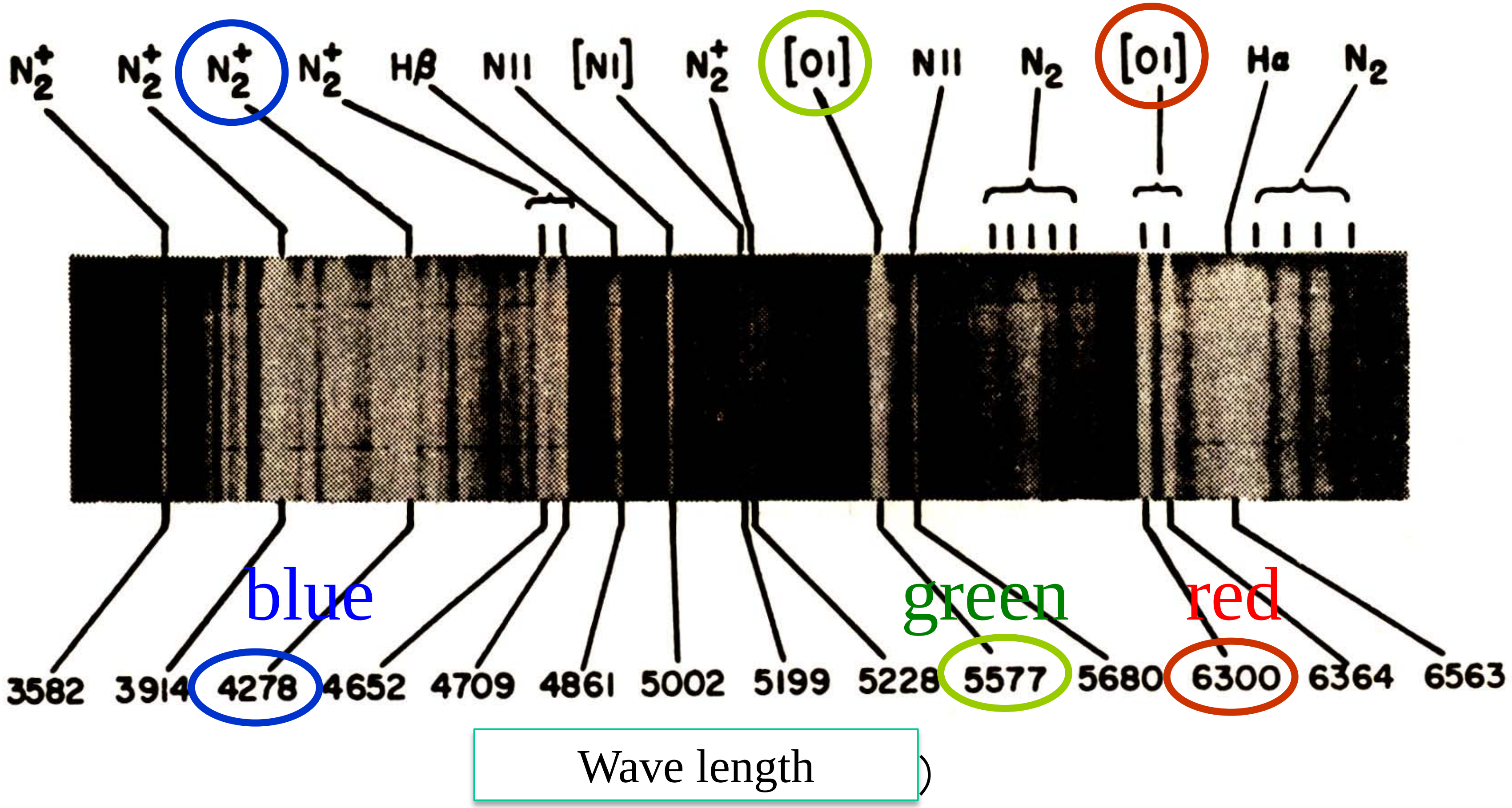

The ‘color’ depending on the amount of energy absorbed and latitudes.

Geomagnetic activity response

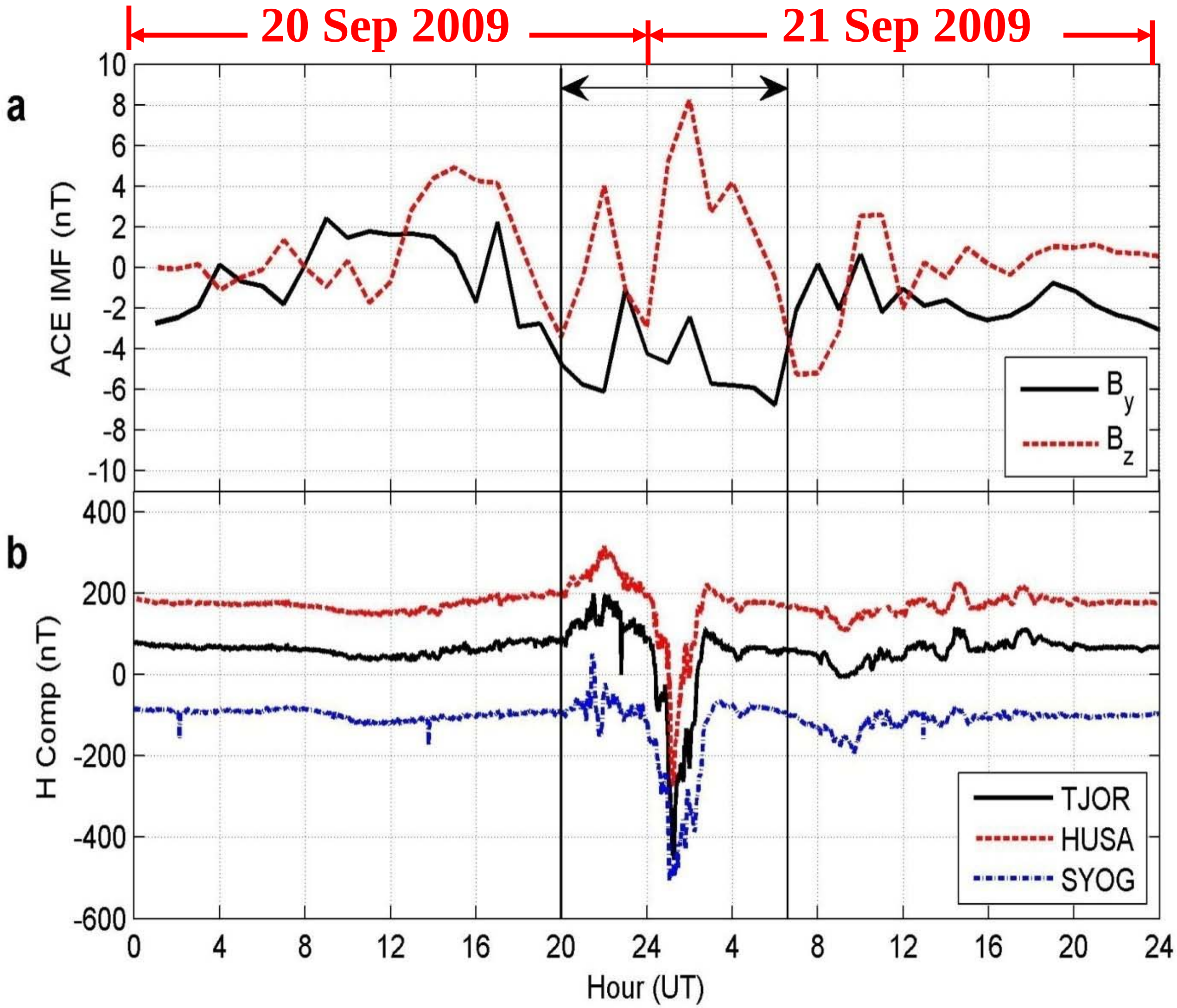

- Magnetic measurements from ACE spacecraft and ground geomagnetic activity (IMF B_y and B_z).
- The disturbance seen at 20:00 UT on 20 Sep ~ 07:00 UT on 21 Sep 2011

Aurora activity on 21 Sep 2009

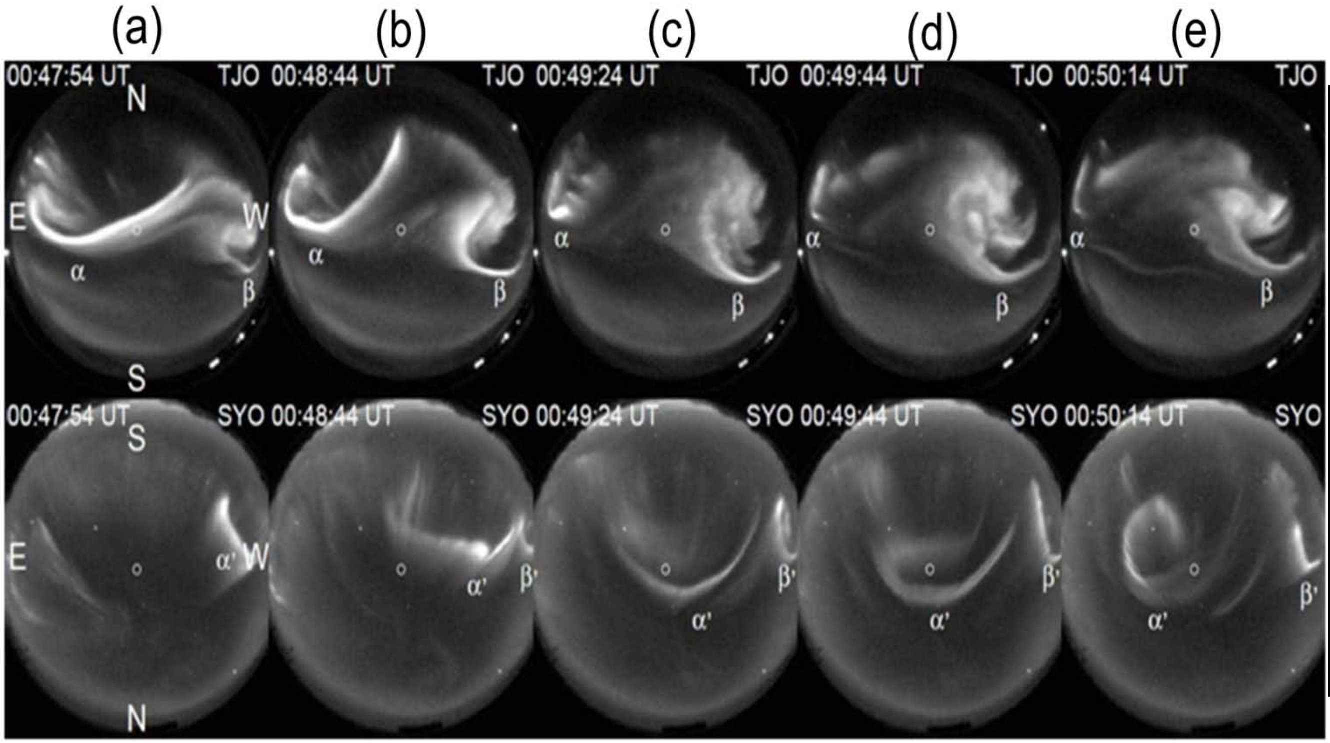

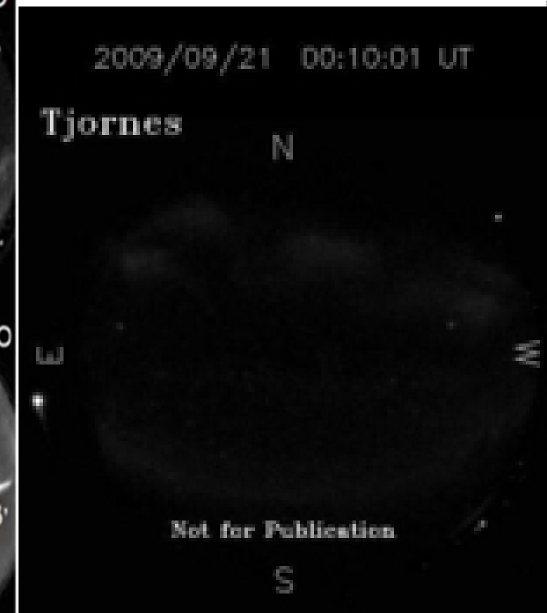

- Looking at the time from 00:47:54 UT to 00:50:14 UT between TJOR and SYOG.
- It is seen that four east-west aligned spiral-like auroral arcs moving eastward in both ASC field of views (FOVs) and each of them had almost a similar form between TJOR and SYOG.

Aurora breakup at conjugate point

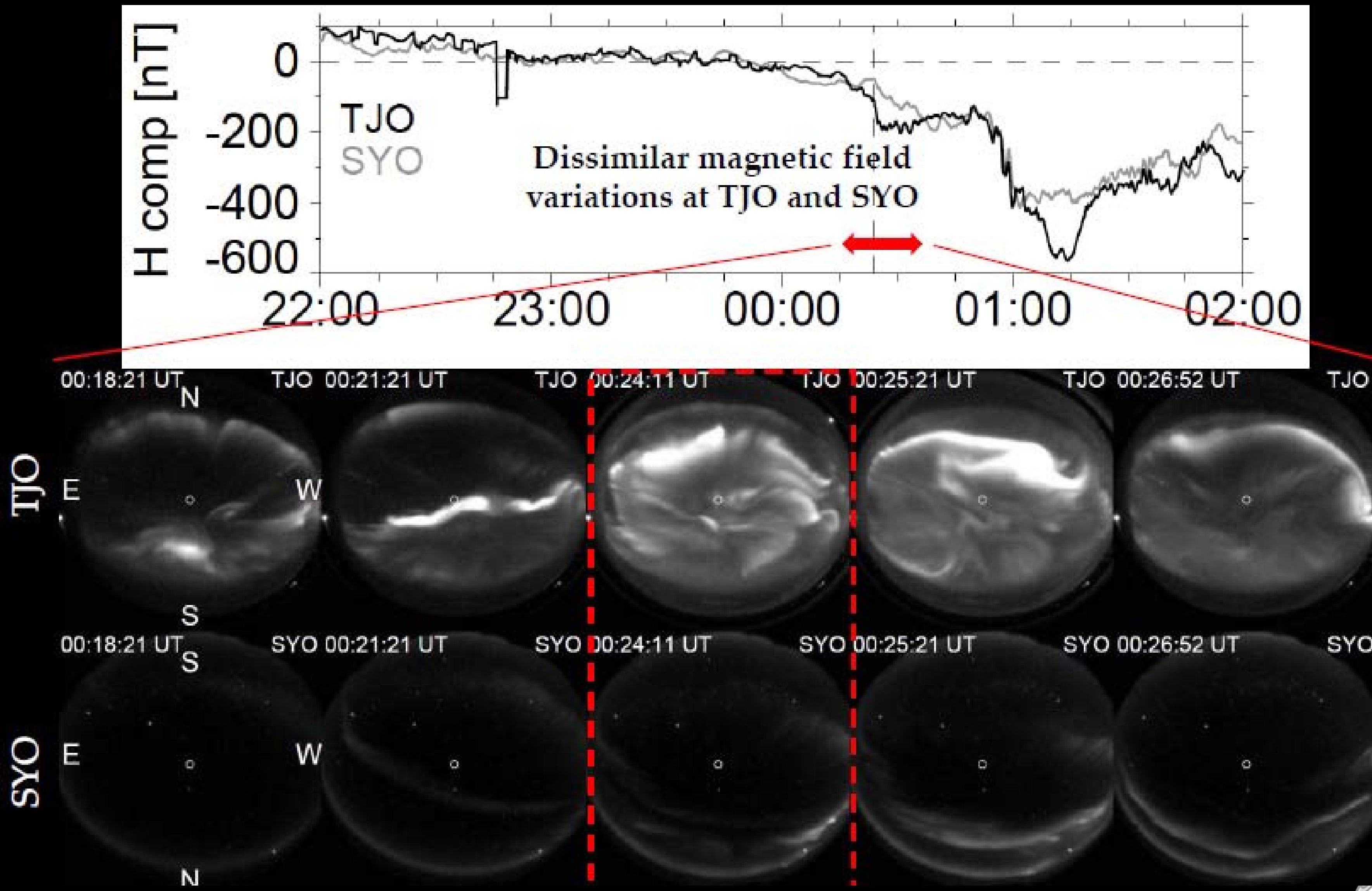

Motoba et al. (JGR 2010)

Keogram – GPS TEC

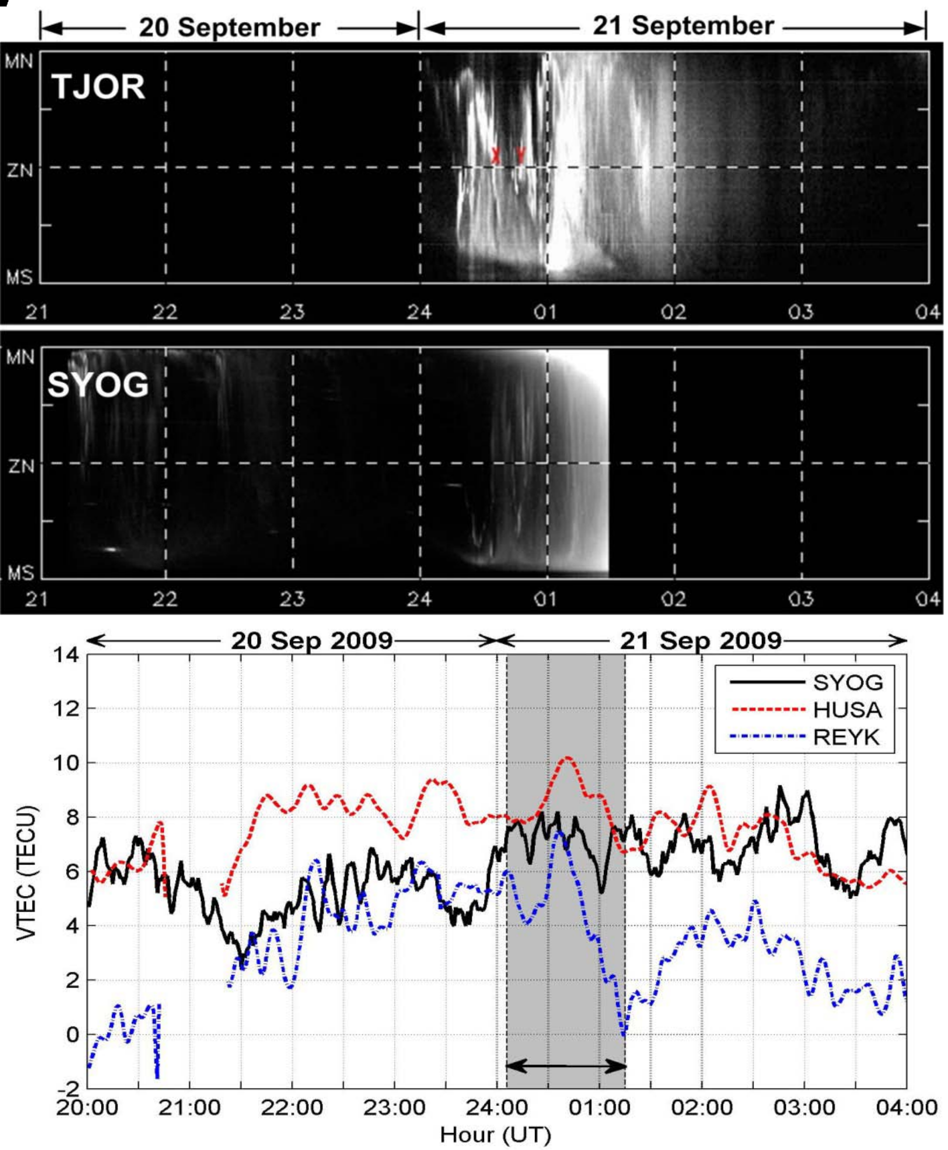

- The conjugate auroras in the late stage of the substorm (after 00:45 UT) between All-sky CCD camera and keogram shows similar features.
- TEC enhancement during a weak substorm can be understood by the enhancement of electron density in the E- and F-regions created by the precipitating auroral electrons associated with the auroral activity.

Height of Aurora

1000 km

300 km

80 km

50km

35 km

15 km

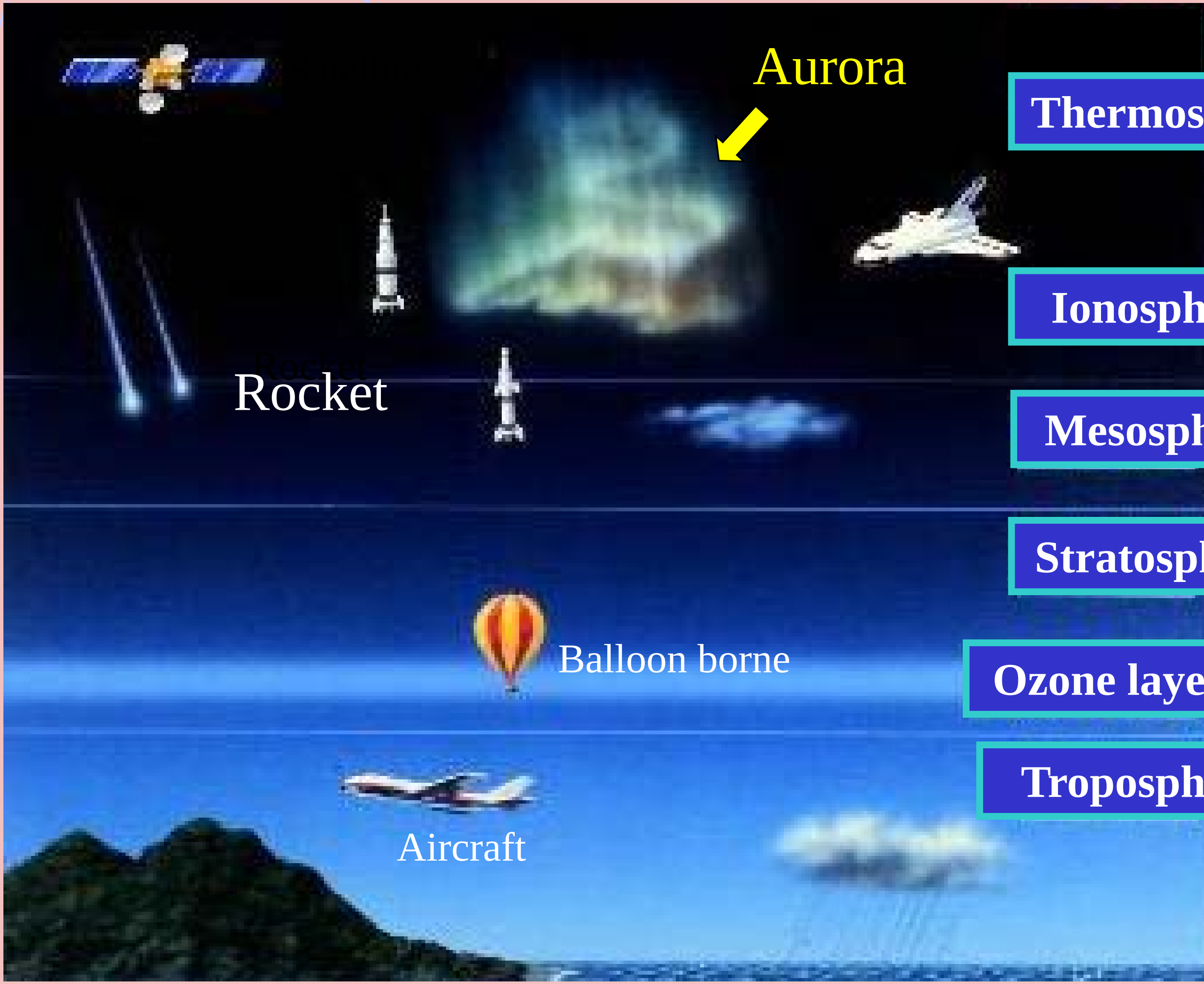

Thermosphere

Ionosphere

Mesosphere

Stratosphere

Ozone layer

Troposphere

How aurora connecting to TEC?

TEC Products

Several products are now available to estimate the TEC every where and at any time.

- Global Ionospheric Maps (GIM): The International GNSS Service (IGS) Analysis Centre (http://igscb.jpl.nasa.gov/components/prods.html) provides VTEC maps. VTEC maps are global maps modeled by using up to 250 globally distributed GNSS stations and using TEC interpolation using spherical harmonics (e.g. Schaer et al., 1998). These maps are estimated every two hours on a 2.5° /5° grid. The CODE Analysis Centre Global Ionospheric Map (GIM), available at ftp://ftp.unibe.ch/aiub/CODE/).
- Klobuchar model: The Klobuchar model (Klobuchar, 1987) is the broadcast Ionospheric Correction Algorithm (ICA) implemented in the GPS system. It is designed to correct for approximately 50% of the ionospheric range delay in GPS measurements . It predicts the VTEC at a given time above a given location.
- IRI 2007 model: The International Reference Ionosphere (IRI) (http://ccmc.gsfc.nasa.gov/modelweb/models/iri_vitmo.php) .This an empirical model based on a wide range of ground and space data (e.g. Bilitza and Reinisch, 2008). It gives monthly averages of electron density, ion composition (O^+, H^+, N^+, He^+, O^+_2, NO^+ and $Cluster^+$), ion temperature and ion drift in the altitude range 50-1500 km in the non-auroral ionosphere.
- Nequick model: This empirical model has been proposed for use in making ionospheric corrections in the single frequency operation of the European Galileo project. It is a quick-run model that allows calculation of the electron concentration at any given location in the ionosphere and thus the TEC along any ground-to-satellite ray-path by means of numerical integration (e.g. Hochegger et al., 2000).